

THE PROTON INVENTORY TECHNIQUE

Authors: **K. S. Venkatasubban**
 Department of Natural Sciences
 University of North Florida
 Jacksonville, Florida
Richard L. Schowen
 Department of Chemistry
 University of Kansas
 Lawrence, Kansas

Referee: W. Wallace Cleland
 Department of Biochemistry
 University of Wisconsin
 Madison, Wisconsin

I. INTRODUCTION TO PROTON INVENTORIES

A. Definition

The term "proton inventory" describes a certain kind of solvent isotope-effect¹ experiment. These experiments, in some cases, lead to a definition of the number of exchangeable protons in the structure of an enzyme or substrate that are *active*, in the sense of being involved in the catalytic mechanism and generating a kinetic or equilibrium isotope effect. In principle, the experiments can yield a list of the kinetic isotope effects at each of the contributing sites: thus, a *proton inventory*.²⁻⁴

B. Measurements²

The experimental procedure is simple. The velocity (or, better, the reaction kinetics) is determined in a series of isotopic water solvents. This series begins with pure protium oxide (HOH) and works up through mixtures with an increasing atom fraction of deuterium to pure, or nearly pure, deuterium oxide (DOD). The result is a compilation of rates or kinetic parameters as a function of the atom fraction of deuterium present in the solvent. The atom fraction of deuterium is sometimes designated by the letter n , as we shall do in this article, and sometimes by x .

C. Interpretation³

The interpretation of the results, in the most straightforward cases, is also facile (Table 1). The form of the curve that relates velocity v_n in each solvent to n , the atom fraction of deuterium, conveys the number of active protonic sites. A linear curve indicates a single site; a quadratic curve two sites, a cubic curve three sites, and so on, culminating in an exponential curve for the "infinite-site" model. The isotope effects at the contributing sites, when small numbers of sites are involved, are determined by fitting the observed function $v_n(n)$ to appropriate equations, like those in Table 1. These formulas are simplified versions of a general equation, the Gross-Butler equation, which will be presented and discussed below. The Gross-Butler equation itself has been known and used since the 1930s and has been extensively tested in simple chemical systems by physical and organic chemists.^{5,6}

D. Mechanistic Significance: Some Examples*1. Trypsin with Bz-Arg-OEt: One-Proton Catalysis⁷*

Frequently the mechanistic implications of a proton inventory are clear from the shape of

Table 1
SIMPLE FORMS OF PROTON-INVENTORY CURVES

One site (one-proton catalysis)

$$v_n = v_o [1 - n + n (k_D/k_H)]: \text{linear}$$

Two sites (two-proton catalysis)

$$v_n = v_o [1 - n + n (k_D/k_H)_1][1 - n + n (k_D/k_H)_2]: \text{quadratic}$$

"Infinite" sites (many-proton catalysis)

$$v_n = v_o (v_1/v_o)^n$$

$$\log v_n = \log v_o + n \log (v_1/v_o): \text{exponential}$$

the function $v_n(n)$, the magnitude of the isotope effects, and other knowledge about the system. If a single protonic site of an enzyme is engaged in proton transfer or in another form of protonic reorganization in the rate-determining step, and if this process contributes the entire solvent isotope effect, then a *linear* ("one-proton") form of $v_n(n)$ is expected. An example of this is shown in Figure 1A. Here the velocity of hydrolysis of Bz-Arg-OEt, catalyzed by trypsin, is plotted against n . The measurements were conducted under conditions where deacylation of the acyl-enzyme, BzArg-trypsin, limits the rate. The linear character shows that the *entire* solvent isotope effect of about 2.8 arises from a single protonic site. Previous work on the mechanism of trypsin action and on acid-base catalysis suggests a model for the origin of this effect. The site which produces the isotope effect is probably a protonic bridge to the active-site histidine imidazole, which acts as a general acid-base catalyst in the deacylation transition state, either by removing the proton of a water molecule attacking the acyl group or by donating a proton to the departing serine oxygen. It is, however, important to note that the proton inventory itself carries no direct information on the structural *location* of the single center that generates the isotope effect. This must be inferred from other knowledge.

2. Asparaginase with Asn: Two-Proton Catalysis⁸

Nonlinear proton inventories are expected if more than one site contributes to the solvent isotope effect, as in any kind of "charge relay" or "proton shuttle" process. Figure 1B shows a case in which $v_n(n)$ is quadratic, indicating that two sites generate the isotope effect ("two-proton catalysis"). These data are for the hydrolysis of Asn catalyzed by the asparaginase of *Proteus vulgaris*. It is thought that formation of an acyl-enzyme limits the rate for V_{\max} here, but this has not been well established. The substrate concentration was several 100-fold in excess of the K_m value so that the velocities are, in fact, essentially equal to V_{\max} . The two-proton character of the proton inventory has been demonstrated by plotting the *square root* of the "partial solvent isotope effect", v_n/v_1 , against n ; since this function is linear in n , v_n itself obviously depends on the second power of n , indicating two-proton catalysis. Furthermore, the linearity of the square-root plot shows that the two contributing sites produce *equal* isotope effects, at least to a rough approximation. The *overall solvent isotope effect*, v_o/v_1 (ratio of rate in HOH to rate in DOD), is about 3.3 so that each site must then contribute the square root of 3.3 or about 1.8. Note that this is the intercept of the proton inventory plot at $n = 0$ when the data are plotted as in Figure 1B. The observation of two-proton catalysis for asparaginase may suggest that it contains some kind of multiproton acid-base catalytic entity, perhaps a charge-relay system of the sort that has been observed crystallographically for the serine proteases, although the proton inventory does not prove this. Crystallographic structures for asparaginases themselves are not yet available. While the asparaginase system appears to operate at the two-proton level (two sites actually involved in catalysis), the data of Figure 1A have shown that this is not the case for trypsin with Bz-Arg-OEt, although the charge-relay system is known from structural studies to exist in trypsin. As we shall see later, the activation of the charge-relay system for catalysis may be a sensitive function of the detailed structure of both substrate and enzyme.

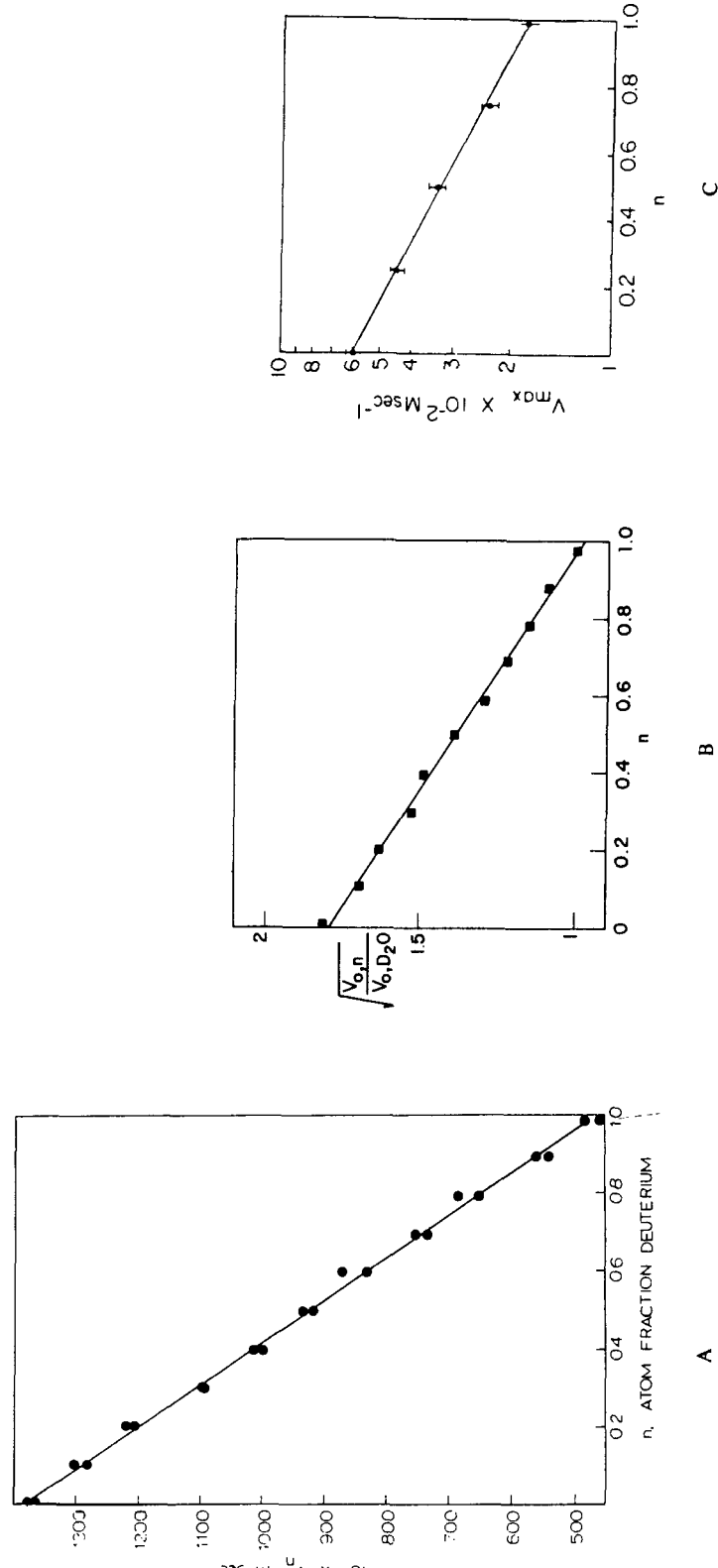


FIGURE 1. (A) Proton-inventory curve for the hydrolysis of Bz-Arg-OEt, catalyzed by trypsin. The velocity, equal to ek_{cat} , is plotted vs. n . The linearity indicates one-proton catalysis. (Reprinted with permission from Elrod, J. P., Hogg, J. L., Quinn, D. M., and Schowen, R. L., Protonic reorganization and substrate structure in catalysis by serine proteases, *J. Am. Chem. Soc.*, 102, 3917, 1980. Copyright 1980, American Chemical Society.) (B) Proton-inventory curve for the hydrolysis of Asn catalyzed by the asparaginase of *Proteus vulgaris*. The square root of the partial solvent isotope effect on V_{max} is plotted against n , so that the linearity of the plot indicates two-proton catalysis. (Reprinted with permission from Quinn, D. M., Venkatasubban, K. S., Kise, M., and Schowen, R. L., Protonic reorganization and substrate structure in catalysis by amidohydrolases, *J. Am. Chem. Soc.*, 102, 5365, 1980. Copyright 1980, American Chemical Society.) (C) Proton-inventory curve for the hydration of carbon dioxide, catalyzed by carbonic anhydrase. The logarithm of V_{max} (n) is plotted against n , so that the linearity of the plot indicates "infinite-site" or many-proton catalysis. (Reprinted from Venkatasubban, K. S. and Silverman, D. N., CO_2 hydration activity of carbonic anhydrase in mixtures of H_2O and D_2O , *Biochemistry*, 19, 4984, 1980. With permission.)

3. Carbonic Anhydrase: Proton Catalysis⁹

If the number of hydrogenic sites along a "proton shuttle" system becomes larger than about five (for overall solvent isotope effects in the range of three to four or less), then the system approaches the behavior of an "infinite-site" model and the proton-inventory curve is exponential. In Figure 1C, such a case is shown. Here the value of $V_{\max}(n)$ is plotted on a logarithmic scale against n . The data refer to the hydration of carbon dioxide, catalyzed by carbonic anhydrase from bovine erythrocytes studied by Venkatasubban and Silverman. The linearity of the plot in this semilogarithmic form shows the proton-inventory function itself to be exponential. The overall isotope effect of 3.2, therefore, arises from a large number of sites, each generating a fairly small isotope effect. The proton-inventory technique, in this limit, can define independently neither the exact number of the sites (beyond specifying it to be "large") nor the exact magnitude of the contribution at each site (beyond specifying it to be "small"). Venkatasubban and Silverman suspect, on the basis of this proton inventory, that the transfer of a proton along a water chain between the active-site imidazole and a zinc-bound hydroxyl group of carbonic anhydrase limits the rate for V_{\max} under these conditions.

E. Limitations

These three examples show how easily proton inventories can be used in straightforward cases. The same examples can be employed to exhibit some of the limitations of the method. The two greatest limitations are (1) the models generated from the proton-inventory data are never unique, although they may be stringently restricted and (2) while the data convey an idea of the number of contributing protonic sites and the isotope effects at each, they cannot (without further investigation) *locate* the contributing sites structurally.

1. Models Not Unique

The nonunique character of proton inventories has been emphasized by Kresge¹⁰ and by Alberly.¹¹ Kresge showed that a linear proton inventory like that of Figure 1A could actually be generated by models involving more than one protonic site. The case in point was the deacylation reaction of acetyl-chymotrypsin, which has an overall solvent isotope effect of 2.4 and a linear proton inventory. It had been concluded from the linearity of the proton inventory that a single site generated the effect and that the charge-relay system was not activated in the deacylation of acetyl-chymotrypsin.¹² Kresge, however, worked out a number of multiproton models that produced linear proton inventories within experimental precision. These models had 2 sites with isotope effects of 1.90 to 1.98 each and from 6 to 20 *other* sites which together give a resultant (inverse) isotope effect of 1/1.51 to 1/1.64.

This appears to be a serious difficulty because it suggests that, in general, a second contributing site may be "hidden" within a linear proton inventory. This concern can be overcome, however, if sufficient data are available. What has been done in Kresge's models is to *pair* the second contributing site with many others that contribute a net inverse isotope effect. Then the resultant contribution of all these extra sites becomes very small, a factor of 1.21 to 1.26. In general, very small isotope effects *and* very small contributions to overall isotope effects are not analyzable by the proton-inventory method. This is because the linear, quadratic, and exponential curves are separated by less than the experimental error in a data point. Thus, it will always be possible to isolate a small contribution (roughly speaking, a factor of less than about 1.5) out of an observed isotope effect and fit any number of contributing sites to it. The requirement for the concealment of the second site within a linear proton inventory is the presence of a number of other sites with a net contribution that completely or nearly completely cancels the contribution of the second site. While this might happen by coincidence in a single case, such cancellation is not likely to be a general phenomenon, across various different substrate structures or enzymes. In fact, the lesson to

be taken is that a proton inventory should form only one part of a larger mechanistic investigation, in which various structures, enzymes, or reaction conditions are examined. Then the probability of any conceivable concealed sites remaining concealed is small.

2. Structural Sources of the Isotope Effects Not Defined

The proton inventory for carbonic anhydrase in Figure 1C serves to illustrate the incapacity of the proton inventory to identify the structural site of the isotope effects. The favored proposal of the authors of this study, that the source of the effect is a chain of water sites linking a zinc hydroxyl ligand and a histidine imidazole of the active site, is very reasonable. It is true, however, that the effect might, in principle, come from other water aggregates more distant from the active site (possibly influenced by an effect transmitted through the protein structure), or the effect might have come from sites in the protein structure, each generating a small isotope effect, perhaps attendant upon a conformation change associated with entering the transition state. Venkatasubban and Silverman were fully aware of this point, and they put their proposal in properly conservative terms.

This limitation, while it should not be allowed to slip from the mind, is shared with a large number of other kinetic techniques. Indeed, the identification and location of the catalytically significant functional groups and other sites in enzymes has been a long-standing general problem, alleviated but not eliminated by protein-structural studies. As the structural information about the enzyme under investigation becomes more refined, and as the detail of mechanistic understanding increases, the number of acceptable sites for interpretation of a particular proton inventory is bound to be narrowed. Furthermore, sometimes the proton inventory itself contains some clear structural clues. For example, the presence of a mechanistically significant sulfhydryl group will lead to a very characteristic contribution to the solvent isotope effect and to the proton inventory.²⁻⁵ This is related to the fact that sulfhydryl groups have an unusual affinity for protium over deuterium, exceeding the relative affinity of bulk water sites by over a factor of 2, while most other protein functional groups have the same relative affinity for deuterium as water itself.

3. Other Problems: pH, Protein Conformation²

Another limitation is the difficulty, referred to already, of interpreting data for very small isotope effects. This can, in principle, be ameliorated by improvements in the precision of kinetic studies, although it is not clear at present that truly great further improvement will be possible.

Some other apparent limitations seem less serious upon careful examination. It is often felt that the problem of pH in DOD-containing solvents will present a problem, but there is no intrinsic difficulty here at all. The control and measurement of pL (the equivalent of pH in mixed isotopic solvents, corresponding to pD in pure DOD) is well understood. So is the correct choice of pLs at which to compare enzymic data, which should correspond to the same effective point on the pL/rate profile. Ordinary electrodes can be employed for pL measurement with no special treatment and with well-established corrections for the effect of deuterium. The subject will not be treated here but has been dealt with extensively in a recent methodological article.² Another concern often voiced is that "heavy water will affect the enzyme." This concern doubtlessly originates in the common knowledge that some protein properties, such as conformation and subunit aggregation, do respond to DOD, sometimes dramatically. However, these responses *are isotope effects*. They are *analyzable* by the proton inventory method. Thus, while it is entirely possible that an observed solvent isotope effect does, indeed, arise from a small or large conformational or other structural alteration, the proton-inventory technique can offer a method of detecting and understanding this. An important fact here is that large structural changes of proteins in DOD compared to HOH are very much the exception, not the rule. A neglected line of evidence showing

this is so is provided by the number of NMR studies of protein structure and dynamics that have been carried out in DOD as solvent. Little or none of the resulting information has emerged as inconsistent with other results obtained in HOH solution.

In summary, the proton-inventory technique offers a convenient and informative approach to elucidating the role of exchangeable hydrogenic sites in enzymic reactions. It is not without limitations. On balance, however, its yield of information in comparison to the required effort and expense is in full accord with the old saw which says that, in scientific work, a trifling investment in fact can produce a handsome return in speculation.*

II. BACKGROUND AND METHODOLOGY

A. Historical Development

1. First Experiments with DOD

Shortly after the discovery of deuterium by Urey et al.^{13,14} on Thanksgiving Day, 1931, the preparation of DOD and its biochemical investigation were launched. Calvin¹⁵ has recalled the activity in G. N. Lewis' laboratory at Berkeley:

The moment that it became clear that a heavy isotope of hydrogen existed, Lewis realized . . . that he probably already had some . . . in the electrolytic cells that Giauque . . . has been using for many years to make liquid hydrogen . . . Lewis began the work by using 20 liters of water from the electrolytic cells . . . and got 0.5 mℓ of water which was about 70% deuterium . . . He took some of his original 0.5 mℓ of D₂O, put it on a petri dish and put some seeds in the petri dish. He also had a control petri dish with ordinary water and the same type of seeds. He watched the development of these seeds. The seeds in the ordinary water sprouted and grew, while the seeds in the heavy water did not; only a few seeds sprouted and grew poorly. Lewis recognized at that time (1933—34) that the deuterium did not kill the seeds, but rather, inhibited their growth.

2. Rule of the Geometric Mean: Gross-Butler Equation

By 1936, Gross and co-workers Krauss, Steiner, Suess, and Wischin at the Chemical Laboratory of the University of Vienna were already publishing a series of papers¹⁶⁻¹⁸ on acid-base phenomena in mixtures of HOH and DOD. These dealt with the acid-catalyzed decomposition of diazoacetic ester,¹⁶ the distribution of picric acid out of isotopic waters into benzene,¹⁷ and the inversion of cane sugar.¹⁸ In the last of these papers, they introduced an assumption critical for the easy use of solvent isotope effects in mechanism chemistry. According to this assumption, the relative abundances of the species HOH, HOD, DOD, and of H₃O⁺, H₂DO⁺, HD₂O⁺, and D₃O⁺ in isotopic waters will be determined solely by statistics and by the ratio of protium to deuterium in the medium. Another statement of this assumption is that the tendency of deuterium rather than protium to enter any site of a molecule is independent of whether deuterium or protium is already found at other sites in the molecule: that there are "no isotope effects on isotope effects." Schwartzenbach¹⁹ independently introduced this assumption in 1938. Gross²⁰ immediately recognized the equivalence of the two formulations (his paper, pointing this out, was now submitted from the University of Istanbul). The assumption has been nearly universally followed in the subsequent practical applications of solvent isotope effects, and is currently known as the Rule of the Geometric Mean (RGM).²¹ In still another independent line of development, Orr and Butler had reached essentially the same point as Gross in their study²² of the "kinetic and thermodynamic activity of protons and deuterons", which appeared in 1937. The use of the RGM led both Gross and Butler to a particularly clear algebraic formulation of the way in which the velocity v_n should depend on n , as a function of the number of contributing sites and the isotope effect at each. As a result, this fundamental expression (somewhat further evolved in form) has become known as the Gross-Butler equation (Table 2).

* Although I am not able to find the source of this remark, I believe it was said by Mark Twain.

Table 2
GROSS-BUTLER EQUATION

$$v_n/v_o = \frac{\prod_1 (1 - n + n\phi_1^T)}{\prod_k (1 - n + n\phi_k^R)} = \frac{\text{TSC}(n)}{\text{RSC}(n)}$$

n = atom fraction of deuterium in mixed isotopic solvent

v_n = velocity in solvent with atom fraction of deuterium n

v_o = velocity in HOH

v_1 = number of protonic sites in transition state

v_k = number of protonic sites in reactant state

Fractionation factors, ϕ

$\phi^i \equiv (X_i^t/X_i^r)/[n/(1 - n)]$

X_D^i, X_H^i = mole fractions of deuterium and protium, respectively, in i th transition-state site

ϕ_j^R for j th reactant-state site

$\text{TSC}(n), \text{RSC}(n)$ = transition-state contribution, reactant state contribution

3. Early Biochemical Work

An astonishing amount of biochemical and biological experimentation with DOD was carried out in the 1930s. Some of this activity seems to have been stimulated by an early report that very small amounts of DOD added to growth media had a great influence on plants.²³ In fact, among the papers from this period is what appears to be the first proton inventory of an enzymic reaction. Following up on an observation that "heavy water can protect epinephrine from destruction by fish scales", Barbour and Dickerson at the Yale Medical School examined in 1939 the effect of DOD on the hydrolysis of acetylcholine bromide, apparently in 0.3 *M* solution, catalyzed by the acetylcholinesterase of dog serum.²⁴ The overall isotope effect was measured as 1.7 (not so different from later findings which will be discussed below), but the rate data were not of high precision and, in fact, do not correspond to a single pH in any of the solvents. The plotted curve of their data is consistent with all models from linear to exponential, so no conclusions can be reached.

4. Modern Developments

The study of reaction mechanisms by use of isotopic solvent mixtures stopped at the beginning of World War II and interest did not return with the end of the war. The two most relevant books of the succeeding period, Bell's *The Proton in Chemistry*²⁵ of 1959 and Melander's *Isotope Effects on Reaction Rates*²⁶ of 1960, do not mention the subject.

The modern history of rates in mixed isotopic solvents begins with a paper by Purlee²⁷ in 1959. According to Gold,⁵ this paper stimulated his own efforts which, along with the extensive studies of Long, Kresge, and their collaborators, laid the groundwork for all current applications. Gold has reviewed the developments of the 1960s in a comprehensive and profound paper that serves well as a fundamental *vade mecum*.⁵ Kresge, in 1964, published a clear and easily grasped derivation of the Gross-Butler equation in the form in which we now employ it, and in the same paper documented the mechanistic utility of the technique.⁶ During the late spring of 1967, C. Behn presented a seminar on Kresge's review to our research group at Kansas. In the ensuing discussions, the idea of applying this technique in a simplified form to enzymic reactions and other related processes began to take shape.

The term "proton inventory" was introduced and defined in a report²⁸ on amide-methanolysis reactions in 1972. The name should not be thought of as a comprehensive designation for all rate measurements in isotopic solvent mixtures. It is better considered as restricted to those cases, such as enzymic reactions, where the complexity of the system precludes the kind of precise definition of all contributions to the solvent isotope effect which is

sometimes possible for reactions of small molecules reacting by simple mechanisms. In the study of relatively simple reactions, great delicacy of interpretation may be reached, and the use of a term as rough and approximate in connotation as “proton inventory” may give (and probably has given) offense.

B. Fractionation Factors: Site-Specific Isotope Effects²⁻⁶

1. Definition

In Table 1, the isotope effects for specific sites were expressed in the usual way, as ratios of rate constants, k_D/k_H . This has disadvantages because a rate constant inevitably links some particular reactant state to some particular transition state. Frequently, it is more useful to think of the transition states and the reactant states, and their individual properties, in independent terms. To permit this, the contribution from a particular site in a particular molecular state is commonly described in terms of an *isotopic fractionation factor*. These factors are readily thought about in the traditional framework of isotope effects and they bear a simple relationship to the rate-constant ratio, which is given by:

$$k_D/k_H = \phi^T/\phi^R$$

where ϕ^T is the fractionation factor for the transition-state site and ϕ^R the fractionation factor for the reactant-state site. Table 2 gives the definition of a fractionation factor as it is used in proton inventories where an average bulk-water molecule is taken as the standard of comparison. Thus, the magnitude of a fractionation factor measures the deuterium preference of a particular site (whether in a reactant or transition state) relative to the deuterium preference of an average bulk-water molecule.

2. Examples

A number of fractionation factors have been measured experimentally, and this further increases their value by providing a set of data against which fractionation factors obtained in proton-inventory fits can be compared. A valuable property of fractionation factors is that they depend on molecular structure only in the immediate neighborhood of the isotopic site. As a result, a given functional group bearing exchangeable hydrogen will tend to have the same fractionation factors, regardless of the molecule in which the group is located. This, in turn, means that we can tabulate, quite briefly, a list of the most important fractionation-factor values and use them as general tools in the interpretation of proton inventories. Lengthy and detailed lists are given elsewhere.² Here we give the ones most useful in enzymic proton inventories in Table 3.

3. Rationale

The key to understanding and remembering the magnitudes of fractionation factors lies in the fundamental rule that governs the distribution of isotopes between different sites at equilibrium: the *heavier* isotope (here deuterium) will accumulate in the site where *binding* at the isotopic center is *strongest*; the *lighter* isotope (here protium) will accumulate in the site where *binding* at the isotopic center is *weakest*; and the greater the difference in binding, the larger the fractionation. Since fractionation factors as defined here measure *deuterium preference* relative to *water as standard*, a large fractionation factor for a site implies that binding at the site is stronger than in bulk water. As it happens, this situation is rarely the case. In a similar manner, a small fractionation factor implies that binding is weaker than in an average bulk-water molecule. As Table 3 shows, this is frequently found.

The values of most of the fractionation factors in Table 3 are not very difficult to understand. Bonds to positive oxygen are weakened relative to those in ordinary water (the standard of comparison) by repulsion between the protonic positive charge and that on the

Table 3
MAGNITUDES OF SOME IMPORTANT CLASSES OF
FRACTIONATION FACTORS²

Type of functional group or bonding situation	Value of fractionation factor	Associated conventional isotope effect
Bonds from hydrogen to neutral oxygen; carbon in sp ² or sp ³ hybridization states; neutral or positive nitrogen	0.8—1.2	1
Bonds from hydrogen to positive oxygen	0.7	1.45
Bonds from hydrogen to sulfur	0.5	2.0
Bonds from hydrogen to sp carbon	0.6	1.7
Ordinary hydrogen bonds between electronegative atoms	1.0	1.0
Hydrogen bonds to oxygen of high basicity (pK ca. 13—18)		
In water solution	0.7	1.4
In the gas phase	0.5	2.0
Transition-state hydrogen bridges in "solvation catalysis"	0.3—0.6	1.5—3
Transition-state hydrogen bridges for proton transfer ^a		
Without tunneling	0.5—0.1	2—10
With tunneling	To 0.05 or less	To 20 or more

^a Most commonly observed for proton transfer among O, N, and S.

^b Most commonly observed for proton transfer to or from C.

oxygen; thus, the factor is less than one. On the other hand, bonds to neutral oxygen are essentially equivalent to those in bulk water, leading to a unit fractionation factor. Bonds to neutral nitrogen are also similar to those to neutral oxygen. Perhaps initially surprising are the bonds to carbon in the tetrahedral (sp³) and trigonal (sp²) states, and to nitrogen when it is positively charged (and is, therefore, also in a tetrahedral, sp³ hybridization state). The stretching motions of the hydrogens in these circumstances do experience weaker binding of the hydrogen (as evidenced by the lower infrared stretching frequencies). However, the addition of further ligands (or in the case of sp² carbon, a pi bond) about the hydrogen-bearing atom apparently leads to a sufficient increase in the effective binding with respect to bending motions of the hydrogen, that the net binding is essentially equivalent to that in a bulk-water molecule. Thus, the fractionation factors are around unity. For hydrogen bound to sulfur, the lowered bending and stretching potentials for motion of the hydrogen attached to this large, polarizable atom combine to generate a weakened net potential and a small fractionation factor. This is of very substantial significance in dealing with enzymic systems in which a sulfhydryl group may be active in catalysis. Finally, for reasons similar to those above (compensation between bending and stretching effects), it appears that in ordinary hydrogen bonds, including those of importance in stabilizing the three-dimensional structure of proteins, the net isotope effects are small and the fractionation factor is, therefore, around unity. In contrast, certain very strong bases, like alkoxide ions, particularly in nonaqueous environments, are capable of bonding the hydrogen in a very shallow potential between the two partner bases. This can lead to quite weak effective binding and small fractionation factors.

The two categories of fractionation factors for transition-state hydrogen bridges correspond to experience in the study of hydrogen-transfer reactions of small molecules. When the transfer of a hydrogen occurs in the rate-determining step, in the sense that the labeled hydrogen has substantial amplitude in the reaction-coordinate motion, then isotope effects of around 2 to 10 are expected (larger when tunneling is important); the corresponding fractionation factors are just the inverse of this value or 0.5 to 0.1. On the other hand, many acid-base catalyzed reactions in which an apparent proton transfer is involved, but in which other processes are also occurring, such as the formation or fission of bonds between atoms of heavier elements than hydrogen (heavy-atom reorganization), do not give such large isotope effects. Values of about 1.5 to 3 are common (fractionation factors of 0.3 to 0.7). The correct explanation for this is not known with certainty, although one possibility (which we have advocated²⁸) is that the labeled center does not participate in the reaction coordinate but rather the hydrogen bridge stabilizes the transition state through a specialized solvation-like interaction ("solvation catalysis").

C. Proton Inventories for Individual Kinetic Constants

1. Multiple Reactant and Transition States

The full form of the Gross-Butler equation for a process in which a single reactant state is transformed into a single transition state is shown as the first expression in Table 2. In principle, the experimentally measurable velocities in isotopic waters, $v_n(n)$, can yield by a process of fitting to the general Gross-Butler expression all of the ϕ^T and all of the ϕ^R — a general and complete proton inventory. This is essentially never feasible in practical studies of enzymic reactions. Still further, one must consider the fact that the measured velocity or rate constant, in most cases, does not correspond to the elementary conversion of a single reactant state into a single transition state.

The first experimental step in addressing this complexity is to obtain proton-inventory data for *individual kinetic constants*. For example, many single-substrate enzymic reactions obey the simplest form of the Michaelis-Menten law:

$$v = e_o k_{cat} S_o / (K_m + S_o)$$

The most informative kinetic constants which can be extracted from this expression are k_{cat} and k_{cat}/K_m . Both of these constants describe the conversion of a single *effective* reactant state into a single *effective* transition state (the word *effective* is important because neither of these states may be, in fact, a single molecular species). Therefore, we can, in principle, write Gross-Butler expressions for k_{cat} and for k_{cat}/K_m individually, but we cannot do this for v , in which the reactant-state and transition-state contributions from the two kinetic constants will be confounded. A Michaelis-Menten analysis must be carried out in each of the mixed isotopic waters (i.e., at each value of n) to obtain $k_{cat}(n)$ and $k_{cat}/K_m(n)$. These may then be considered in terms of a Gross-Butler expression, although even this is subject to further constraints introduced below.

2. Weighting-Factor Approach

Often a procedure in which one of the usual analyses (e.g., nonlinear least-squares analysis of $v[S]$) is used to obtain the kinetic parameters is less effective than an alternative scheme of Stein.²⁹ In this scheme, the velocities at each value of n are measured in paired experiments, in which a value of v_o , the rate in HOH at the same substrate concentration, is measured along with v_n . Then the experimental result can be expressed as an *observed isotope effect*, v_n/v_o or v_o/v_n . The observed effect is related as follows to the partial solvent isotope effects on each of the kinetic parameters:

Table 4
ILLUSTRATIVE DERIVATION OF WEIGHTING FACTORS FOR COMMON KINETIC LAWS*

Random, sequential bireactant

$$\begin{aligned} 1/v_n &= AB/(V_m/\alpha^n K_A^n K_B^n) + A/(V_m/\alpha^n K_A^n) + B/(V_m/\alpha^n K_B^n) + 1/V_m^n \\ v_o/v_n \equiv n_v &= {}^n(V_m/\alpha K_A K_B)w_{ab} + {}^n(V_m/\alpha K_A)w_a + {}^n(V_m/\alpha K_B)w_b + {}^nV_m w_v \\ w_{ab} &= v_o \alpha^n K_A^n K_B^n / V_m^n AB \\ w_a &= v_o \alpha^n K_A^n / V_m^n A \\ w_b &= v_o \alpha^n K_B^n / V_m^n B \\ w_v &= v_o / V_m^n \end{aligned}$$

Ping-pong bireactant

$$\begin{aligned} 1/v_n &= A/(V_m^n/K_{mA}) + B/(V_m^n/K_{mB}) + 1/V_m^n \\ v_o/v_n \equiv {}^n v &= {}^n(V_m/K_{mA})w_a + {}^n(V_m/K_{mB})w_b + {}^nV_m w_v \\ w_a &= v_o K_{mA}^n / V_m^n A \\ w_b &= v_o K_{mB}^n / V_m^n B \\ w_v &= v_o / V_m^n \end{aligned}$$

* Kinetic laws taken with slight modification from Segel, H., *Enzyme Kinetics*, Wiley-Interscience, New York, 1975, 275 (sequential) and 608 (ping-pong); conditions are initial forward velocities in the absence of products.

$$(v_o/v_n)^{-1} = w_k(k_{cat}^n/k_{cat}^o)^{-1} + w_{k/K}[(k_{cat}/K_m)^n/(k_{cat}/K_m)^o]^{-1}$$

$$w_k = S/(S + K_m^o)$$

$$w_{k/K} = K_m^o/(S + K_m^o) = 1 - w_k$$

Adopting the Northrop notation³⁰ for isotope effects, we write for any kinetic parameter p , ${}^n p \equiv p^o/p^n$. Thus

$${}^n v = w_k^n k_{cat} + (1 - w_k)^n (k_{cat}/K_m)$$

The observed isotope effect is, thus, a weighted average of the desired partial solvent isotope effects on the kinetic parameters. The weighting factors, w_k and $w_{k/K}$, describe the degree of saturation of the enzyme *in pure HOH solvent*. This is an important point: the weighting factors are the *same in every mixed isotopic solvent* — they derive from a knowledge of the value of K_m in *HOH alone*. Furthermore, the resulting isotope effects on the kinetic parameters, calculated from this equation, are very insensitive to the exact value used for K_m , variations of 10 or 20% or more often being without significance. Thus, the desired partial solvent isotope effects can be obtained by plotting against w_k the reciprocal of observed solvent isotope effects, v_o/v_n , at various substrate concentrations in a single isotopic solvent. The plot will be linear; the intercept at zero gives ${}^n(k_{cat}/K_m)$, the intercept at unity gives ${}^n k_{cat}$. Only a relatively undemanding determination of K_m in HOH solvent alone is necessary to calculate the needed values of w_k .

The same kind of treatment can be applied to more complex kinetic laws. Table 4 shows examples of the weighting factors appropriate to commonly encountered kinetic laws. When more than two kinetic constants are involved, no such plot as the one described above can be used. A general least-squares computer program can, however, be employed to get partial solvent isotope effects for each of the kinetic parameters. The weighting factors necessary again derive from a reasonably easy kinetic analysis for HOH alone.

D. Multiple Rate-Determining Steps and Reaction Channels

In specific cases, it will be accurate to represent the data, even for a particular kinetic

parameter, in terms of a simple Gross-Butler equation only if a single reactant state and a single transition state are actually kinetically significant in determining the parameter. Otherwise a more complex expression is required.

For example, suppose that k_{cat}/K_m is not equal either to a rate constant for simple binding of substrate to the enzyme, nor to one for a subsequent chemical step, but rather that both contribute to determining this kinetic constant. Then its value, in terms of the binding rate constant k_b , the equilibrium constant for binding K_s , and the rate constant for the chemical step k_c , is

$$(k_{cat}/K_m)^{-1} = (k_b)^{-1} + (K_s k_c)^{-1}$$

At this point, we can introduce a Gross-Butler expression for each of the constants k_b and $K_s k_c$. Using the notation TSC_b and TSC_c for the respective transition-state contributions $[\Pi_i^y(1 - n + n\phi_i^T)]$ and noting that the reactant-state contributions, $RSC [\Pi_i^y(1 - n + n\phi_i^R)]$, is the same for the two rate constants, we have:

$$(k_{cat}/K_m)^{-1} = \{[TSC_b(n)k_b^0]^{-1} + [TSC_c(n)k_c^0]^{-1}\}[RSC(n)]$$

Then, for the partial solvent isotope effect, we have

$$^n[k_{cat}/K_m] = [RSC(n)]\{w_b[TSC_b(n)]^{-1} + w_c[TSC_c(n)]^{-1}\}$$

$$w_b = [k_{cat}/K_m]^0/k_b^0$$

$$w_c = [k_{cat}/K_m]^0/K_c^0$$

Here the values of the weighting factors are not readily accessible from experimental data, as were those in the case of the observed isotope effects above. These weighting factors here have to be obtained from information about the kinetic significance of the two contributing steps. They are usually treated as parameters of the fit and determined along with the isotope effects. Again, however, they refer to the situation only in HOH and are the same in each isotopic solvent mixture.

A treatment similar to the one above can be constructed for any combination of serial or parallel processes contributing to a given kinetic parameter. Table 5 shows the appropriate weighting schemes.

In general, one will not know in advance whether more than one step contributes to determining the value of a kinetic parameter, so that the proper formulation for the Gross-Butler treatment will not be known. Various possibilities must be tried with both the weighting factors and fractionation factors, as noted above, treated as adjustable parameters. The proper Gross-Butler formulation and the associated mechanism are one of the conclusions that can sometimes be drawn from a proton inventory study.

E. Shapes of Common Proton-Inventory Curves³

After collection of the observed isotope effects, in order to select possibly appropriate mechanistic models, the form is examined of a plot of v_n vs. n for each of the kinetic parameters in order to decide what the most probable formulations are to test as models for representing the data. A plot of v_n vs. n commonly has one of three possible general shapes: linear, bowl-shaped ("holds water", bulging downward), and dome-shaped ("spills water", bulging upward). Some examples of these are shown in Figure 2, and a summary of the possibilities that are commonly encountered is given in Table 6.

Table 5
WEIGHTING FACTORS FOR SERIAL AND PARALLEL STEPS

Serial steps

Particular $k_n^{-1} = k_{an}^{-1} + k_{bn}^{-1}$
 $k_i/k_n \equiv {}^n k = w_a {}^n k_a + w_b {}^n k_b$
 $w_a = k_i/k_{an}; w_b = k_i/k_{bn}$
 General ${}^n k = \sum w_i {}^n k_i$
 $w_i = k_i/k_{in}$

Parallel steps

Particular $k_n = k_{an} + k_{bn}$
 $({}^n k)^{-1} = w_a ({}^n k_a)^{-1} + w_b ({}^n k_b)^{-1}$
 $w_a = k_{an}/k_n; w_b = k_{bn}/k_n$
 General $({}^n k)^{-1} = \sum w_i ({}^n k_i)^{-1}$
 $w_i = k_{in}/k_n$

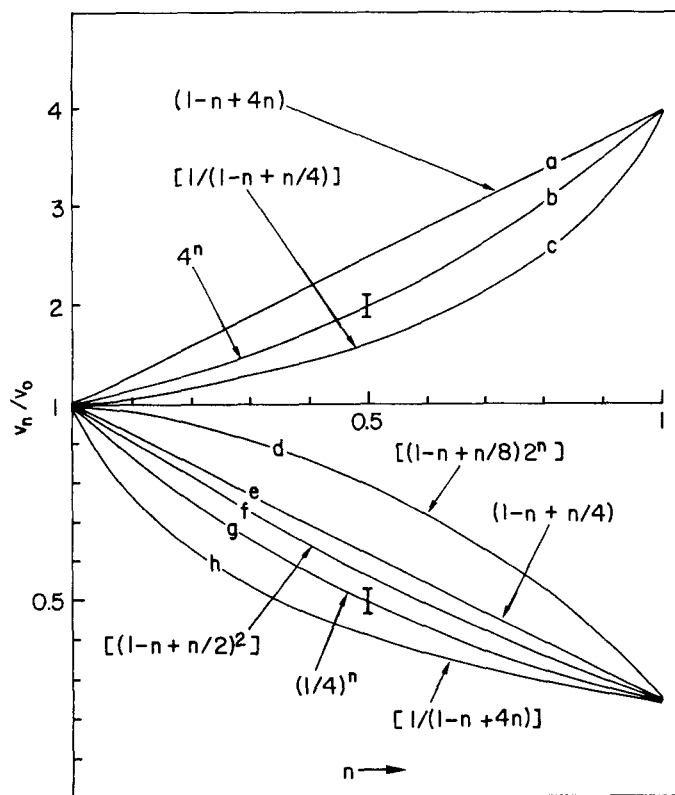


FIGURE 2. Some typical shapes of proton-inventory curves. The mechanistic models for the three upper curves correspond to: (a) one "tight" transition-state site with $\phi^{\ddagger} = 4$; (b) many sites experience a tightened potential as the transition state is formed, leading to an overall inverse solvent isotope effect of 4; (c) a single "loose" reactant-state site with $\phi^R = 0.25$. The models for the remaining, lower curves all generate a normal overall solvent isotope effect of 4. The mechanisms correspond to: (d) one transition-state site which gives an isotope effect of 8 (as in a proton-transfer reaction), opposed by a many-site inverse contribution of 2 (as from a conformational change); (e) a single transition-state site produces $k_H/k_D = 4$; (f) two transition-state sites each produce an isotope effect $k_H/k_D = 2$; (g) many sites are "loosened" as the transition state is formed, giving the overall normal effect of 4; (h) a single very "tight" reactant-state site with $\phi^R = 4$ is loosened in the transition state so that $\phi^{\ddagger} = 1$. The error bars shown on curves (b) and (g) correspond to $\pm 5\%$. (Reprinted from Schowen, K. B. and Schowen, R. L., *Methods Enzymol.*, 87C, 551, 1982. With permission.)

Table 6
COMMON SHAPES OF PROTON INVENTORY CURVES AND THEIR SIGNIFICANCE

Linear: single transition-state site
Linear inverse: $v_n^{-1}(n)$ linear: single reactant-state site
Bowl-shaped ("holds water")
Polynomial (curvature smaller than exponential): multiproton
Exponential ($\log [v_n]$ linear): "infinite-proton"; many sites contribute small individual isotope effects; "medium effect"
Complex models (curvature greater than exponential or unsatisfactory fit to polynomial functions)
More than one reaction channel: at least one must be multiproton, otherwise curve is linear
More than one rate-determining step in series: bowl-shaped only under special conditions
Dome-shaped ("spills water")
Combination of normal and inverse contributions (particularly indicated if $v_n(n)$ exhibits a maximum)
More than one rate-determining step in series

The nonuniqueness of the models that fit a particular curve has to be reemphasized. The guidelines for selecting appropriate models, provided by Figure 2 and Table 6, must be considered always in the context of other mechanistic information.

The simplest result is a *linear plot*. For this case, this situation is straightforward and the most direct interpretation is that the effect arises wholly from one site in the transition state. The isotope effect (or the fractionation factor) is readily calculated from the slope of the plot. If the effect is an acceptable one in the context of other mechanistic knowledge, it is unnecessary to go farther.

Sometimes the plot of v_n against n is itself nonlinear, but when the reciprocal velocities are plotted, a linear function results. One interpretation of this behavior is that the Gross-Butler equation has the form:

$$v_n^{-1} = v_o^{-1} (1 - n + n\phi^R)$$

This corresponds to all $\phi_i^T = 1$ and all $\phi_j^R = 1$ except for the single ϕ^R seen in the equation. In this case, the effect arises from a single site in the *reactant* state, for which ϕ can again readily be obtained from the slope of the reciprocal plot. Whether this is the correct interpretation has to be judged on the basis of the quality of the reciprocal linear fit and the appropriateness of the concept and isotope effect in terms of the mechanism.

Bowl-shaped plots generally signal the contribution of more than a single site. Simple models take these multiple sites to be present in a single combination of one reactant state and one transition state — that is, the model assumes that a single step, along a single-reaction channel, determines the rate. Most simply, the shape of the curve fits a polynomial function:

$$v_n = a_0 + a_1n + a_2n^2 + \dots + a_vn^v$$

This is what one would obtain by expanding the Gross-Butler equation for v contributing sites in the transition state:

$$v_n = v_o \prod_i^v (1 - n + n\phi_i^T)$$

In principle, the isotope effects could be fit to the polynomial equation and the fractionation factors calculated from the coefficients $a_0, a_1, a_2, \dots, a_v$ so obtained. In practice, this is

rarely a workable procedure. A better strategy is to use the polynomial fit to estimate the most likely number of sites and then to obtain the ϕ values by fitting directly to the appropriate Gross-Butler equation. For example, one can try fitting the data to successively higher-order polynomials until some statistical test (e.g., the Fisher F-test) indicates that the addition of further terms to the polynomial is no longer statistically justified. This gives the maximum number of sites that can be claimed from the proton-inventory data. In actual cases, two, three — or possibly with large isotope effects — four sites are about as far as the procedure can be carried. Then the different curves become indistinguishable within the error limits of the data.

The terminal point of increasing curvature in the bowl-shaped plots, as the number of contributing sites increases, is the so-called “infinite-site” or “medium effect” model. This arises if a very large number of sites each contributes a very small isotope effect and these multiply together to produce an effect of the observed magnitude. Under these conditions, the plot becomes exponential and $\log(v_n)$ is linear in n . This can readily be understood by recalling that

$$1 - n + n\phi = 1 + n(\phi - 1) = \exp[n(\phi - 1)] = [\exp(\phi - 1)]^n$$

if ϕ is very close to unity, i.e., if the isotope effect at the site in question is very small. For a large number Q of such sites,

$$(1 - n + n\phi)^Q = \{\exp[Q(\phi - 1)]\}^n = Z^n$$

where the total isotope effect Z may be quite large. This kind of proton inventory is expected if (1) there is a chain of protonic sites in the solution or the enzyme structure with each site contributing an isotope effect; (2) the isotope effect arises from solvation changes (thus, “medium effect”); (3) the isotope effect arises from rather nonspecific alterations in protein structure.

Sometimes bowl-shaped proton inventories exhibit *more* than an exponential degree of curvature (i.e., the observed points lie below a plot of $[v_1/v_0]^n$). Such observations cannot be accounted for by a multisite model involving only one reactant state and one transition state. For a bowl-shaped curve, the most probable complex model, involving more than one reaction process, is a multichannel model. For example, two parallel reactions may be proceeding at once. However, if both channels are one-proton channels, the shape will still be linear:

$$v_n = v_{01}(1 - n + n\phi_1) + v_{02}(1 - n + n\phi_2)$$

$$(v_n/v_0) = 1 - n + n(v_{01}/v_0)\phi_1 + (v_{02}/v_0)\phi_2$$

$$(v_n/v_0) = 1 - n + n(w_1\phi_1 + w_2\phi_2)$$

If one of the contributing pathways has a multiproton mechanism, however, then a bowl shape comes about. The curvature of such a plot can be large and can exceed exponential curvature.

In principle, two steps in succession which both contribute to determining the rate will give a nonlinear proton inventory even if both have one-proton mechanisms. The expected form of such a plot is dome-shaped. However, if the isotope effects on the two processes and their weighting factors have the right relationships, an overall bowl shape can, nevertheless, result (it is often “baggy”: the rate drops slowly at low n , and then much more rapidly at high n). Such models, thus, also must be considered for bowl-shaped curves.

For *dome-shaped* proton inventories, the contribution of more than one serial step to determining the rate is one reasonable explanation. A second explanation is that there is a competition between inverse solvent isotope-effect contributions, tending to make the rate faster in DOD, and normal isotope-effect contributions, tending to make the rate faster in HOH. The result is a dome shape. In fact, this kind of circumstance can even produce maxima in the proton-inventory plot.

Qualitative examination of the plots and trial fits to the data can, in this way, suggest to the experimenter the best functions to pursue in modeling. The procedures recommended here are the ones we commonly employ. A valuable, different approach has been recommended by Alberty¹¹ and is used by some important groups in the field. This is known as the "gamma method". It is very straightforward to apply in practice, although the relationship of the quantity γ , the central parameter, to physical quantities is algebraically complicated. Readers who wish to use this method should consult the original treatment.¹¹

F. Fitting Models to Data

Once one or more models have been selected, by whatever procedure, it is commonly desired to extract the values of the fractionation factors, i.e., the isotope effects at the individual sites, from the experimental data. This is achieved by a fit of the model equation to the data.

Any general least-squares procedure can be used for fitting. We employ the BMDP computer package, which is available in most computer centers. It is simple to use and provides good statistical analyses of the fit and the parameters in its output. It is not unusual to find, for reasonably complex models, that substantial correlation exists between parameters of a model. This results in large standard deviations for the parameters corresponding to high values of the covariances. Sometimes, if there is independent information that allows some of the parameters of the models (e.g., fractionation factors or the weighting factors for individual reaction channels or rate-determining steps) to be fixed in advance, then the standard deviations of the remaining parameters can be reduced.

Often one wishes to compare the quality of fit for two or more competing models in order to select the best. Generally, the important considerations are the fraction of the variation in the data which is accounted for by a given model, and whether there is any systematic character to the residual deviations of the experimental points about the calculated function for a given model. The first quantity, fraction of total variation accounted for, is readily obtained from standard fitting programs. The second question can be answered, as Gandour and co-workers³¹ have emphasized, by plotting the residuals against n . The best result is that the distribution of these residuals should be random, with zero mean. If this is untrue, and particularly if there is a clear systematic character to the pattern of residuals, it suggests that the model being fitted is incorrect. Thus, the ideal model produces the minimum residual variance and a random distribution of residual deviations about zero.

III. CASE HISTORIES

A. Serine Proteases

1. Structure, Mechanism, Specificity, and Efficiency³²⁻³⁴

A considerable amount of proton-inventory work concerning the serine proteases has appeared. To facilitate its discussion within the context of general mechanistic knowledge about these enzymes, some of their features will be reviewed in the briefest manner. There are books and reviews which treat this subject in detail.³²⁻³⁴

Figure 3 shows a schematic diagram³⁴ of the active site of chymotrypsin, with the most important structural regions and their mechanistic significance indicated. The other serine proteases share much of this structure and a good many of the more remote structural

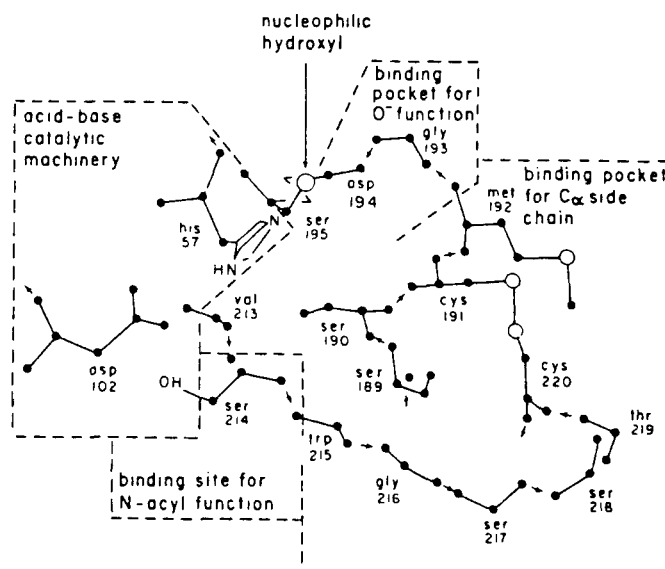


FIGURE 3. Schematic diagram of the active site of chymotrypsin. (Reprinted from Hegazi, F., Quinn, D. M., and Schowen, R. L., *Transition States of Biochemical Processes*, Gandour, R. D. and Schowen, R. L., Eds., Plenum Press, New York, 1978, chap. 10. With permission.)

characteristics of chymotrypsin, the major distinction arising in the specificity pocket, which binds the C_{α} side chain at the scissile residue (the one at which the amide bond is hydrolyzed) to the substrate polypeptide chain. The differing structure in this pocket confers the characteristic individual specificity patterns on the members of the serine proteases family, as will be mentioned below for each enzyme. Here, we shall concentrate on those features of the active site which are of special concern in interpreting proton-inventory studies.

The central characteristic of the serine proteases is the nucleophilic serine hydroxyl group, from which the enzyme family takes its name. In the apparently absolutely general "double-displacement" mechanism, this group is initially acylated by the substrate in what appears to be a standard carbonyl-displacement reaction. The amino-bearing leaving group is liberated and an intermediate acyl enzyme is generated. In a second reaction stage, the acyl enzyme, an ester, undergoes hydrolysis. The active enzyme is regenerated and the carboxylate product is set free.

Intrinsically, the serine is neither a reactive nucleophile nor a good leaving group in its acylated form. The enzyme possesses several features which seem to have been designed to accelerate both the initial acylation step and the subsequent deacylation step. The most interesting of these features employs a form of protonic catalysis and, thus, may generate solvent isotope effects. These two preeminent catalytic devices are (1) the charge-relay system (catalytic triad; acid-base catalytic entity), and (2) the oxyanion hole.

The charge-relay system is the chain of hydrogen bonds (or potential hydrogen bonds) leading from the nucleophilic serine to the imidazole of His-57, to the carboxylate of Asp-102, and conceivably farther into the enzyme structure. It was first identified in X-ray structural studies by Blow et al.³⁵ and has been a subject of controversy ever since. The name "charge-relay system" relates to the concept that the relay of a positive charge along a chain of hydrogen bonds from or to a center of developing or diminishing electron density might give more effective catalysis than its transport to or from a closer position. A number of structural studies have by now shown that this kind of relay of the proton does not occur

in titration of resting states of the enzymes, nor in protonation of the phosphorylated derivative of trypsin.^{36,37} The latter was assumed to be a model of the tetrahedral adducts that may be intermediates in the carbonyl displacement reactions.³⁷

The lack of such function in resting stages is in general agreement with various ideas about enzyme catalysis,^{32,38,39} all of which emphasize the importance of the release of stabilizing energy in the transition state, but its conservation in stable states (so that a differential stabilization of the transition state and, thus, catalysis occurs). The proton-inventory method then suggests itself as a means of investigating the situation in the transition state.

The oxyanion hole is a set of two N-H bonds so situated as to be able to function as hydrogen-bond donors to the negative oxygen of the substrate or acyl-enzyme carbonyl group in the transition states for acylation or deacylation. In these transition states, this oxygen will be more negative than in any of the stable carbonyl species because of partial bonding of other atoms to the carbonyl carbon. If the N-H bonds are aligned for specially effective interaction or if the nearby environment particularly promotes such a stabilizing interaction, then the oxyanion hole may promote the reaction over that in aqueous solution. If these protonic interactions produce isotope effects, they will influence proton inventories. Mechanistic experience in small-molecule systems suggests that the charge-relay system is a more probable source of isotope effects than the oxyanion hole. As will be seen below, we interpret observations on the serine proteases in terms of the charge-relay system, not in terms of the oxyanion hole, and we believe this likely to be correct. In complete rigor, however, the oxyanion hole as a source of the observed isotope effects cannot be definitely excluded at present.

In addition to the C_α side-chain binding pocket, a number of subsites also exist (designated S₂, S₃, etc., for interaction with peptide residues P₂, P₃, etc.). Interactions between substrate structure and enzyme structure at these "remote" subsites are known to affect differential stabilization of the transition states. One of the subsite features is seen in the figure, that for the first N-acyl function along the "polypeptide tail" of the acyl fragment of the substrate.

2. Chymotrypsin^{7,10,12,40}

In chymotrypsin, the specificity pocket is just that shown in Figure 3. Its structure is such as to favor reasonably large, hydrophobic side chains like those of Phe, Trp, or Leu. Proton inventories have been employed with chymotrypsin to approach the questions:

- How many protonic sites are involved in catalysis?
- Does this number or the magnitude of the associated isotope effects depend on the structure of the substrate?

Clearly, the first of these questions is aimed at the function of the charge-relay system. Since it has long been known that the enzymic activity is reduced in DOD by two- to fourfold, some form of acid-base catalytic component is indicated. The number of sites involved would distinguish ordinary acid-base catalysis (one site) from charge-relay catalysis (multiple sites).

The second question arises from concern about the degree to which interactions between parts of the substrate structure and parts of the enzyme structure, in the catalytic transition state, may be *responsible for the function* of the acid-base catalytic apparatus, whether it has the character of a charge-relay system or not. Data available at the present time do not fully resolve these questions for chymotrypsin, but they provide some suggestive leads.

Proton-inventory studies for some substrates show that, at least under some circumstances, chymotrypsin can function as a *one-proton catalyst*: charge-relay catalysis is not in operation. For example, consider the data shown in Figure 4. In these plots, the partial solvent isotope

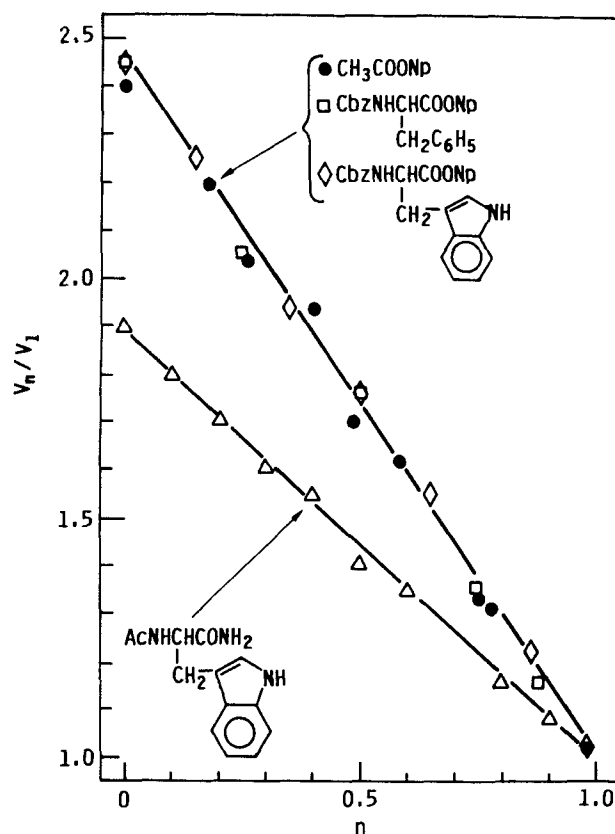


FIGURE 4. Proton-inventory curves illustrating one-proton catalysis by chymotrypsin.

effect v_n/v_1 is plotted against n . The plots are visually linear, and this is confirmed by statistical analysis (quadratic terms are not significant above the 90% confidence limit). Such a result corresponds to generation of the isotope effect by a single transition-state site.

For three of the substrates (upper line), which are *p*-nitrophenyl esters, the rate-limiting step is deacylation of the acyl enzyme, the partial solvent isotope effects being values of $k_{\text{cat}}^n/k_{\text{cat}}^1$. Remarkably, the data for all three substrates fit exactly the same line: the overall solvent isotope effect (2.45) and the proton inventories are identical. Furthermore, the structures of the three substrates differ considerably. The acetyl substrate is a *minimal* substrate, capable of interaction with the enzyme only at the actual center undergoing covalency change. On the other hand, the other two are *quasispecific* substrates: they possess both the *N*-acyl group and the C_α side chain which fills the specificity pocket. Thus, in addition to the interactions at the center of covalency change, these two substrates add interactions in the specificity pocket and at the *N*-acyl binding site. Nevertheless, the isotope effect is unaffected and the proton inventory corresponds to a single site.

The lower line in the figure is for Ac-Trp-NH₂, a quasispecific substrate for which the acylation step is rate limiting. The overall isotope effect here is similar although somewhat smaller (1.9). Again the proton inventory is linear. Thus, no sign of charge-relay catalysis is seen for the acylation step, either, even when the interactions at the specificity pocket and the *N*-acyl binding site are present.

The proton inventories cannot indicate the structural site in the enzyme which is producing

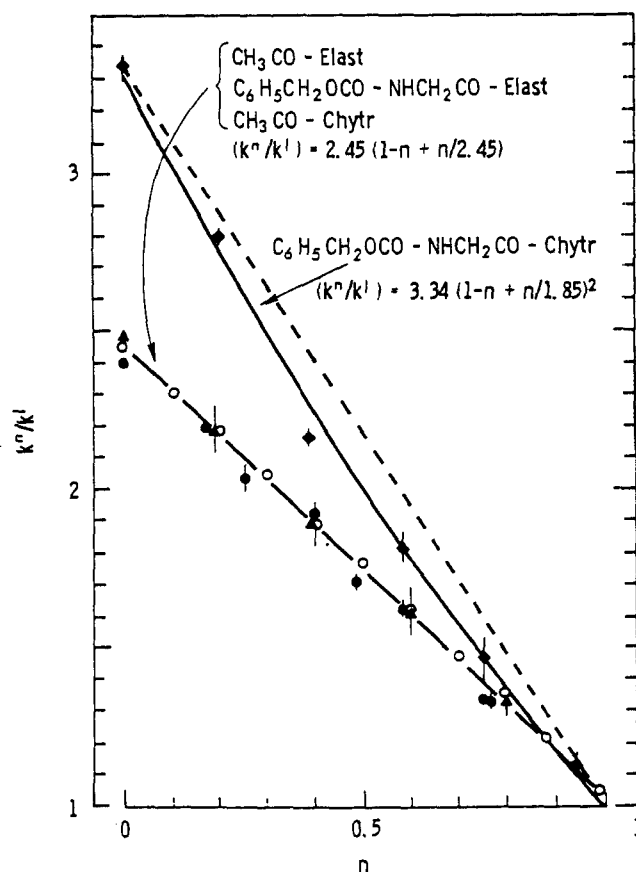


FIGURE 5. Proton-inventory curve illustrating two-proton catalysis by chymotrypsin (upper line). The lower, one-proton line is for Ac-ONp with both chymotrypsin and elastase and for Cbz-Gly-ONp with elastase.

the isotope effect of 1.9 to 2.5. The most logical hypothesis is, of course, that the imidazole ring of His-57 is acting as a simple general acid-base catalyst, both in acylation and deacylation.

Excellent experimental models in small-molecule chemistry have been provided for such a situation by Hogg and collaborators. The imidazole-catalyzed hydrolysis reactions of acetylimidazole and of ethyl trifluorothiolacetate have overall solvent isotope effects of 3.32 and 2.84, respectively. Their proton inventories, measured by Patterson et al.,⁴¹ are linear so that the effect arises from a single site, presumably a hydrogen bridge to the catalytic imidazole. The magnitude of these isotope effects somewhat exceeds the range for the chymotrypsin cases described above, but as we shall see, there is a considerable range of one-proton isotope effects in the serine-protease series. It encompasses the magnitudes for these and other model reactions.

It is tempting to conclude that the charge-relay system never operates as such. This would be wrong, as the data of Figure 5 indicate. The lower, straight line in Figure 5 corresponds to data for Ac-ONp with chymotrypsin (also shown in Figure 4) and for two deacylation reactions of the related serine protease, elastase. All exhibit one-proton catalysis with an overall solvent isotope effect of 2.45. The upper curve, however, is different. These data are for the deacylation reaction with Cbz-Gly-ONp as substrate; the overall effect is now 3.34 and the proton inventory indicates two-proton catalysis.

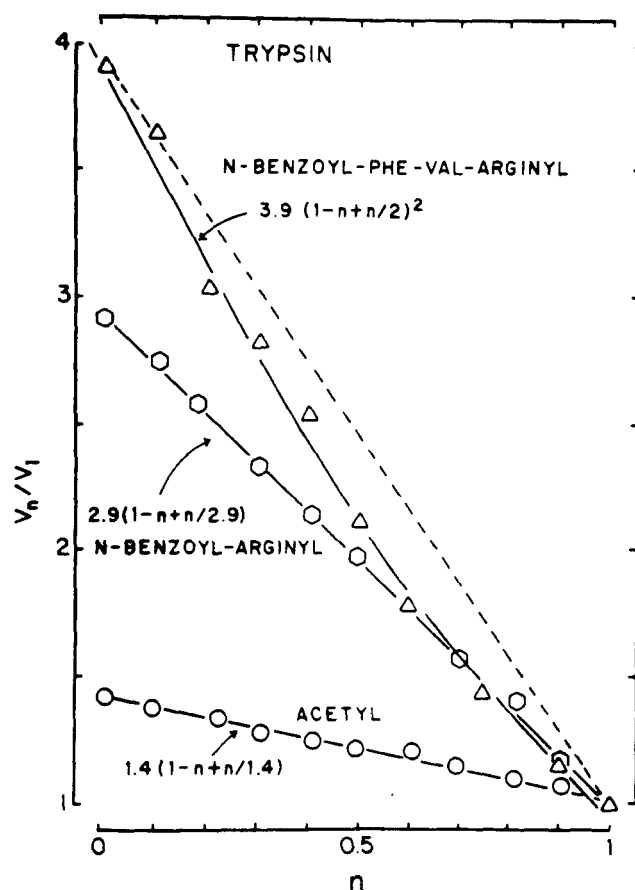


FIGURE 6. Proton-inventory curves for trypsin catalysis.

The combined results for Figures 4 and 5, therefore, present a complicated picture. Minimal interaction between enzyme and substrate, as with acetyl groups, leads to one-proton catalysis. Thus far, quasispecific substrates with interaction at both C_α and N -acyl subsites *also* produce one-proton catalysis. In a single case, the presence of an N -acyl but not a C_α interaction has led to two-proton catalysis (with chymotrypsin but not elastase).

A tentative hypothesis holds that sufficient numbers and types of subsite interactions can activate the charge-relay apparatus, leading to two-proton (or multiproton) catalysis. Short of this full sufficiency, however, a given set of interactions may or may not produce activation, depending on the exact structures, of both enzyme and substrate, which are involved.

3. Trypsin⁷

Trypsin is a serine protease closely related to chymotrypsin, but with a specificity pattern that favors a positively-charged C_α side chain at the scissile residue. This preference arises from a difference in structure of the two enzymes, trypsin having a negatively charged residue at the base of the specificity pocket, where chymotrypsin has a neutral residue.

Figure 6 shows proton-inventory results for three substrates of trypsin. They are, in a general sense, compatible with the observations for chymotrypsin, but there are important differences. The three substrates are Ac-ONp (deacylation rate-determining), Bz-Arg-OEt (deacylation rate-determining), and Bz-Phe-Val-Arg-NHNp. The last substrate, an oligo-

peptide *p*-nitroanilide, probably has the acylation step as rate-limiting, but this is not known with certainty.

In contrast to the situation with chymotrypsin, Ac-ONp shows a quite small isotope effect of 1.4. This is smaller than is commonly observed in well-defined model systems for one-proton general acid-base catalysis and is too small for accurate proton-inventory analysis. It suggests that the general-base catalyzed reaction of serine with the acyl group of the substrate does not actually determine the rate, but that rather some other event which does not involve protonic catalysis is wholly or partially rate limiting. One possibility, which is purely speculative, is that the His imidazole of the active site operates as a *nucleophile*, rather than as a protolytic catalyst with this minimal substrate. Such a role was earlier suggested by Hubbard and Kirsch⁴² for chymotrypsin with phenyl benzoates as substrates. The only firm statement possible at this point, however, is that the effect is unusually small. Bz-Arg-OEt is a quasispecific substrate of trypsin, carrying the correct C_α side chain for the specificity-pocket interaction and the requisite *N*-acyl function for binding at the corresponding subsidiary site. As with chymotrypsin, the proton inventory is linear and the catalysis, thus, appears to involve a single site in the transition state. The magnitude of the overall isotope effect, 3.0, is larger than for the various one-proton cases with chymotrypsin.

The oligopeptide substrate possesses the correct C_α side chain and *N*-acyl function at the scissile residue and, in addition, possesses two further residues for interactions with the remote subsites, S₂ and S₃ (some degree of interaction of the benzoyl function with S₄ might also occur). Now the isotope effect is further increased, to a value around 4, and the proton inventory is strongly nonlinear. A two-proton model yields individual isotope effects at the two contributing sites of around 2.

The observation of two-proton catalysis with an oligopeptide substrate, which possesses residues not only for interaction at the active site but also at more remote sites, now begins to confirm the hypothesis introduced for chymotrypsin, where the effects of binding at subsites on the charge-relay system were unpredictable. The oligopeptide result here suggests that the presence of further interactions at the remote subsites, along with C_α and *N*-acyl interactions, leads to full function of the charge-relay system. A good approximation to the structure of the evolutionarily anticipated substrate brings the system into action; fragments of this structure may or may not activate it.

4. Elastase^{7,40,43,44}

Two different kinds of elastase have been examined by the use of proton inventories. Porcine pancreatic elastase⁴³ (PPE) has the specificity pocket modified so as to prefer an Ala residue at the scissile position, while human leukocyte elastase⁴⁴ (HLE) prefers Val.

Figure 7 shows the situation with PPE for, in effect, four different substrates.^{7,40,63} This upper curve in Figure 7 fits data⁷ for Ac-ONp. The data⁴⁰ for Cbz-Gly-ONp, shown in Figure 5, fall on the same line. With PPE, the minimal substrate Ac-ONp behaves precisely as it does with chymotrypsin. The overall isotope effect is 2.45 and arises from a single site in the transition state. The addition of an *N*-acyl function to produce Cbz-Gly-ONp, however, in contrast to the situation in chymotrypsin, does *not* activate two-proton catalysis. Instead, the isotope effect remains at 2.45 and the effect continues to come from one site only. For both substrates, the data are for k_{cat} , so that deacylation is rate-limiting.

The lowest curve in the figure is for Cbz-Ala-ONp, which combines the *N*-acyl function with the correct C_α side chain. As with chymotrypsin, the combination of these two features does not activate the multiproton catalytic machinery (the proton inventory is linear). However, the overall isotope effect does not remain the same as with minimal substrates, but is reduced to 1.75. These data are for the acylation step (k_{cat}/k_m).

The middle curve⁴³ is for an oligopeptide *p*-nitroanilide, Ac-Ala-Pro-Ala-NHNp. The identity of the rate-limiting step with the *p*-nitroanilide substrate is not known with certainty,

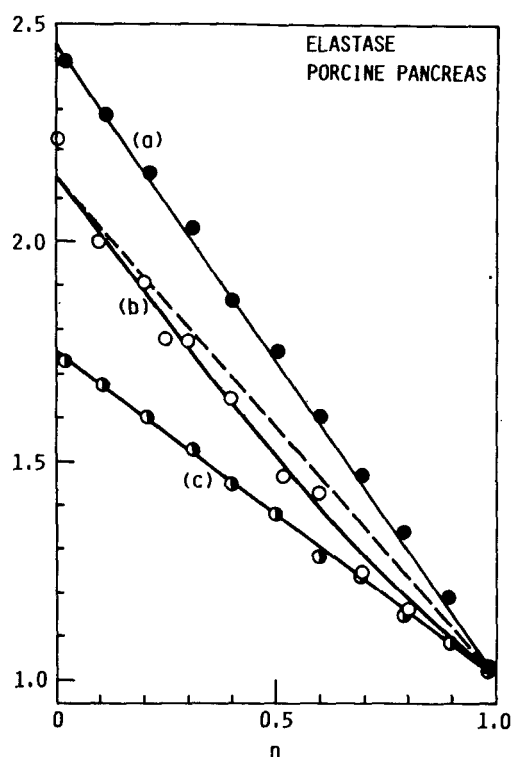


FIGURE 7. Proton-inventory curves for the action of porcine pancreatic elastase. (a) Ac-ONp, 25°, pH 7.50, 0.03 M Tris buffer; $k_{cat}^n = k_{cat}^1 (2.45)^{(1-n+n/2.45)}$. (b) Ac-Ala-Pro-Ala-NHNp, 25°, pH 8.75, 0.1 M Tris buffer; $k_{cat}^n = k_{cat}^1 (2.15)^{(1-n+n/1.47)^2}$. (c) Cbz-Ala-ONp, 25°, pH 8.00, 0.05 M Tris buffer; $(k_{cat}/K_m)^n = (k_{cat}/K_m)^1 (1.75)^{(1-n+n/1.75)}$.

although rate-limiting acylation has been suggested. In any case, the oligopeptide substrate, as with chymotrypsin and trypsin, once again exhibits two-proton catalysis. The overall isotope effect is 2.15, corresponding to 1.47 at each of the two sites for which the curve in Figure 7 is drawn.

Stein⁴⁴ has conducted studies with HLE which show that even an oligopeptide structure, if it is without the correct C_α side chain, is not capable of activating the charge-relay system with this enzyme. In fact, a correct choice of the residue even at P₂ may also be necessary for activation. His results relate to three substrates (recall that specific substrates for HLE require Val at the scissile bond):

$$\text{Suc-Ala-Ala-Ala-NHNp: } {}^{\text{DOD}}k_{cat} = 2.15; {}^{\text{DOD}}(k_{cat}/K_m) = 2.59$$

$$\text{Suc-Ala-Ala-Val-NHNp: } {}^{\text{DOD}}k_{cat} = 2.71; {}^{\text{DOD}}(k_{cat}/K_m) = 2.19$$

$$\text{MeOSuc-Ala-Ala-Pro-Val-NHNp: } {}^{\text{DOD}}k_{cat} = 3.34; {}^{\text{DOD}}(k_{cat}/K_m) = 1.43$$

Stein has suggested that K_m may be a true dissociation constant for the first two substrates, so that the small difference in the overall solvent isotope effects on the two kinetic parameters (about 20%) may be a physical isotope effect on the binding, similar to an isotope effect on solubility. If this is so, then acylation must determine the rate for both kinetic parameters with these substrates and HLE.

Proton inventories for these three compounds are shown in Figure 8. The observations were made at substrate concentrations of $3 K_m$, $0.05 K_m$, and $10 K_m$ for the three substrates in the order listed above. They do not, therefore, correspond to proton inventories of completely "pure" kinetic constants but to weighted averages of 75% k_{cat} , 95% k_{cat}/K_m , and 90% k_{cat} , respectively.

The curves are fully linear for the first two substrates. The charge-relay mechanism is, thus, not activated and the isotope effect arises from a single site, in spite of the fact that both substrates provide occupation of subsites S_1 , S_2 , S_3 , and to some degree S_4 , with the second substrate providing the evolutionarily preferred side chain at S_1 . Finally, for the third substrate, with the addition of one more residue, neutralization of the terminal succinate, and the placing of a Pro residue at P_2 , the full charge-relay function enters. As shown in the inset, the square-root plot is linear.

Actually, since several changes in structure were introduced simultaneously in proceeding to the last substrate, we cannot at this point know which are crucial. As Stein wrote, "Although we can define for some cases substrate structural requirements, at this time we are still unable to predict the structural features that will result in the intimate and precise transition-state interactions necessary for coupling and full functioning of the charge-relay system."

5. α -Lytic Protease^{43,45-48}

α -Lytic protease is, in many ways such as its specificity pattern, similar to the elastases. It is, however, of bacterial origin and contains only one histidine. This has made it the centerpiece of NMR studies connected with the charge-relay system.⁴⁶⁻⁴⁸ Because it is produced in bacteria, the enzyme can be obtained with the single histidine labeled with either C-13 or N-15 by the straightforward expedient of feeding the bacterium with the correspondingly labeled amino acid in culture. This was, in fact, done. C-13 and N-15 NMR methods were then used to determine whether acidic titration of the enzyme would place the proton that is added around pH 7 on the histidine imidazole (expected on the basis of ordinary pK values, but considered in contradiction to the charge-relay hypothesis) or, instead, would relay it through to the aspartate carboxyl, contrary to the ordinary expectation for the relative pKs, but a result that would seem to confirm the charge-relay concept.

Some confusion resulted, with the carboxylate⁴⁶ first being claimed as the final resting place of the proton, then the imidazole.⁴⁷ The current upshot favors the imidazole.⁴⁸

While these structural studies are perfectly relevant to a complete understanding of serine-protease catalysis, they have no significance for the question of charge-relay function in the catalytic transition state. What they do suggest is that *if* the charge-relay chain has a catalytic (i.e., transition-state) function involving its protonic sites, then this function is not commonly observable in accessible ground states of the enzyme. Its function must, therefore, be restricted to the transition state. This is, of course, just what is expected for an effective enzyme.^{32,38,39} A good enzyme brings its stabilizing capacities into action *specifically* in the transition states, and only there. Expression of such binding in other states would reduce catalytic activity and is, thus, not expected.

The available proton-inventory data for α -lytic protease, which constitute a direct probe into the transition-state situation, again provide a contrast between the minimal substrate Ac-ONp, incapable of subsidiary interactions with the enzyme, and the extended substrate Ac-Ala-Pro-Ala-NHNp. The data refer to somewhat different circumstances: k_{cat}/K_m at pH 8.1 for Ac-ONp and k_{cat} at pH 8.8 for the oligopeptide *p*-nitroanilide. The results are somewhat similar to those for other serine proteases and are not shown in graphical form.

The oligopeptide shows the larger overall effect (2.78) and a bowl-shaped proton inventory which fits a two-proton model. The isotope effect at each of the two sites is 1.67. Since α -lytic protease prefers Ala at the scissile residue, this is extremely similar to the other cases of specific oligopeptides. Two-proton catalysis, charge-relay function, appears to be indicated.

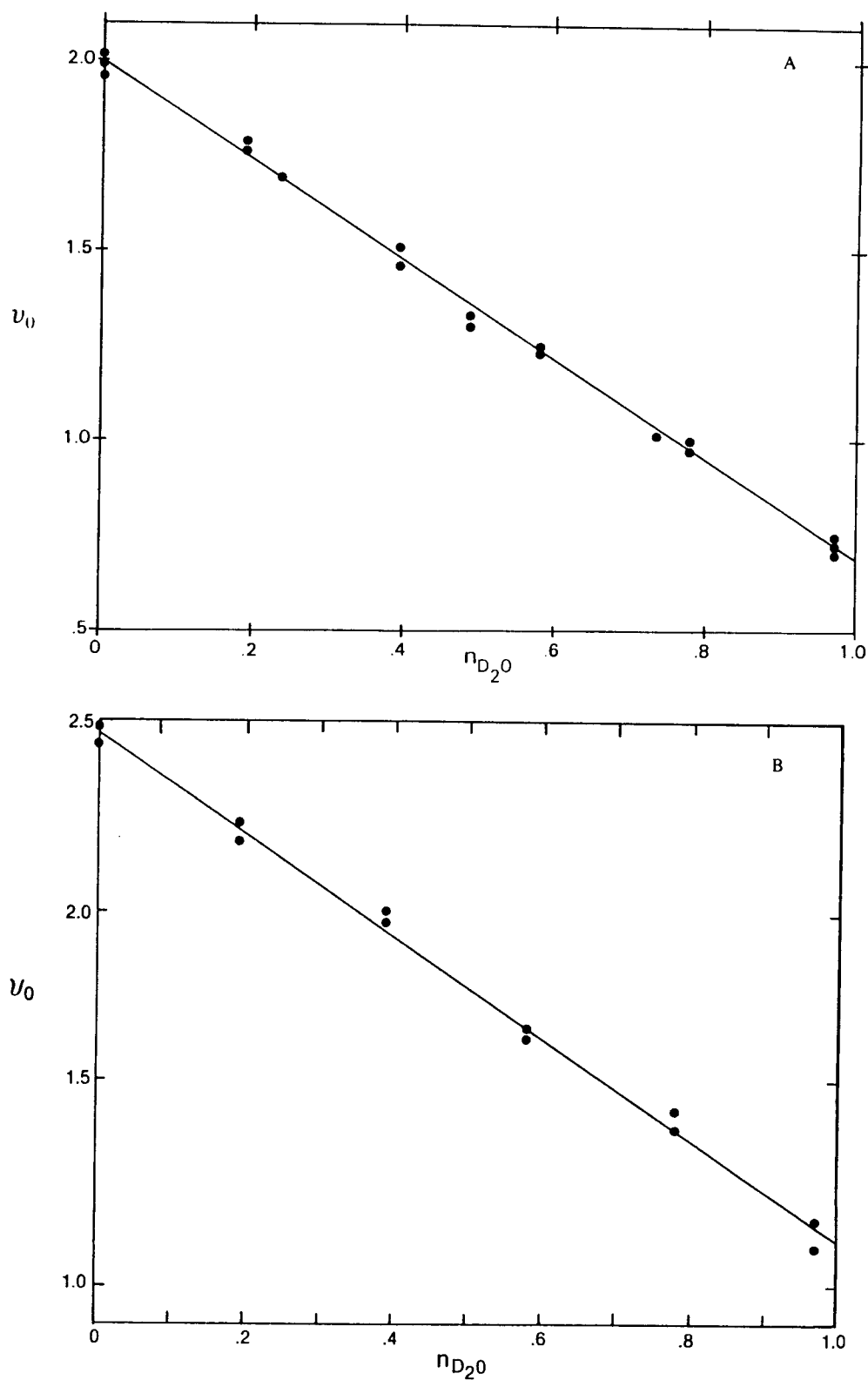


FIGURE 8. Proton-inventory curves for the action of human leukocyte elastase. (A) Suc-Ala-Ala-Ala-NHNp (k_{cat}/K_m); (B) Suc-Ala-Ala-Val-NHNp (k_{cat}/K_m); (C) MeOSuc-Ala-Ala-Pro-Val-NHNp (k_{cat}).

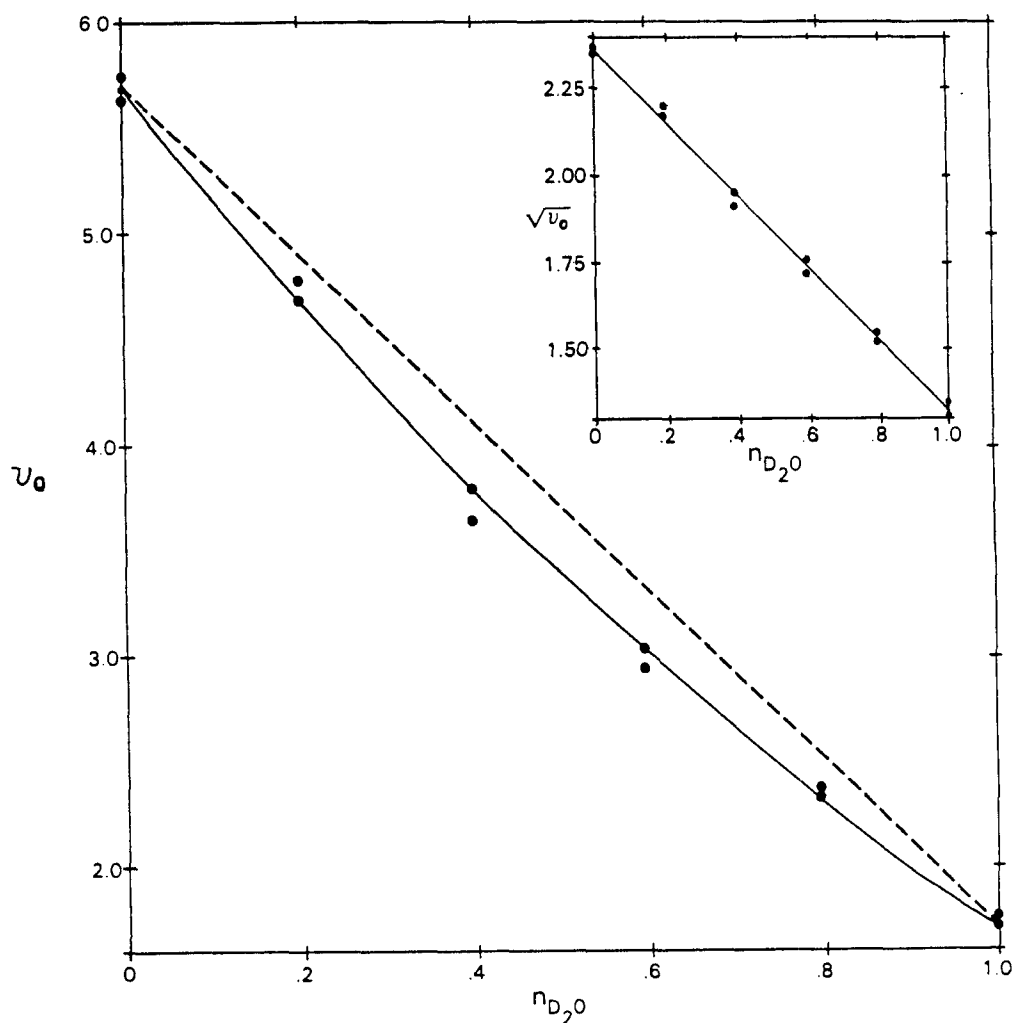


FIGURE 8C

The minimal, acetyl substrate shows a dome-shaped curve. One possible explanation for such a curve is competition between inverse and normal isotope-effect contributions. A fairly extensive mechanistic hypothesis based on this interpretation has been given⁴⁵ and will not be repeated here. Another possible interpretation is that the dome shape derives from a change in rate-determining step with two kinetically significant transition states in series. In fact, a good fit to the data can be calculated from the equation:

$$(K_{cat}/K_m)_n/(K_{cat}/K_m)_1 = 2.10\{0.25 + [0.75/(1 - n + n/2.45)]\}^{-1}$$

This corresponds to one step with no isotope effect and a weighting factor in HOH of 0.25, and a second step with a weighting factor of 0.75 and a one-proton isotope effect of 2.45. This second step could, of course, be the "chemical step" generating such a one-proton isotope effect, as was observed with chymotrypsin and elastase. The first step might be a simple "physical step" of binding, which contributes no isotope effect. At the moment, no evidence permits a choice among this and other possible hypotheses.

Table 7
SUMMARY OF PROTON INVENTORY STUDIES FOR SERINE PROTEASES

Enzyme	Substrate	Kinetic parameter	Overall isotope effect	No. of sites	Ref.
Chymotrypsin	Ac-ONp	k_{cat}	2.45	1	12
	Cbz-Phe-ONp	k_{cat}	2.45	1	65
	Cbz-TrpONp	k_{cat}	2.45	1	65
	Ac-Trp-NH ₂	k_{cat}	1.90	1	7
	Cbz-Gly-ONp	k_{cat}	3.34	2	40
	PhCH ₂ CH ₂ CO-ONp	k_{cat}	2.85	1	7
Trypsin	Ac-ONp	k_{cat}	1.4	1?	7
	Bz-Arg-OEt	k_{cat}	3.03	1	7
	Bz-Phe-Val-Arg-NHNp	k_{cat}	4.00	2	7
Elastase (PP)	Ac-ONp	k_{cat}	2.45	1	7
	Cbz-Gly-ONp	k_{cat}	2.45	1	40
	Cbz-Ala-ONp	k_{cat}/K_m	1.75	1	66
	Ac-Ala-Pro-Ala-NHNp	k_{cat}	2.15	2	43
Elastase (HL)	Suc-Ala-Ala-Ala-NHNp	k_{cat}	3.15	1	44
	Suc-Ala-Ala-Val-NHNp	k_{cat}	2.71	1	44
	MeOSuc-Ala-Ala-Pro-Val-NHNp	k_{cat}	3.34	2	44
α -Lytic Protease	Ac-ONp	k_{cat}/k_{cat}	2.10	*	45
	Ac-Ala-Pro-Ala-NHNp	k_{cat}	2.78	2	43

* Dome-shaped curve.

6. Summing Up for the Serine Proteases

The serine proteases have yielded up the three major classes of *forms* for proton inventory curves: linear, bowl-shaped, and dome-shaped. So far, bowl-shaped curves corresponding to multiproton catalysis, and, thus, probably to the effective function of the charge-relay catalytic machinery, have been found for each of the enzymes studied (chymotrypsin, trypsin, elastase, and α -lytic protease) with what might be termed *sufficiently specific* substrates. By this is meant those which display a sufficient number of the evolutionarily anticipated structural features of the natural substrate. The actual structural requirements vary considerably, as is emphasized by the summary presented in Table 7.

Linear curves, corresponding to one-proton catalysis, are generated by substrates of *insufficiently* specific structure in most cases. In one case, Ac-ONp with α -lytic protease, a dome-shaped curve resulted when k_{cat}/K_m , corresponding to rate-limiting acylation, was examined. (There are preliminary indications⁴⁵ of a similar shape for acylation of chymotrypsin by Ac-ONp, also.) The dome shape has several conceivable explanations (combinations of inverse and normal isotope effects, changes in rate-determining step), among which no confident choice can be made. The linear cases produce single-site isotope effects in the range expected from model reactions for a simple one-site general acid-base catalysis.

Considered together, the entire data seem to us to suggest that the charge-relay apparatus of the enzyme is susceptible of activation through an extensive set of enzyme-substrate interactions, involving not only those at the scissile residue, but also those at remote subsites. When these interactions are absent, the enzyme functions as a simple one-site general catalyst. The activating interactions may have an internally balancing, or conflicting character so that not only the correct interaction at one site, but the correct *combination* of interactions at various sites is required for the reliable activation of the catalytic machinery.

We suspect that this is one manifestation of a general phenomenon.⁴⁰ In this view, enzymes and their substrates experience mechanical alterations of structure, which are mutually brought

about in both enzyme and substrate as the two enter the catalytic transition state together. Here, the activation of the charge-relay system may be brought about by structural compression of the entire hydrogen-bond chain, as a result of attractive interactions between the residues along the polypeptide tail of the substrate and the appropriate subsites of the enzyme. The substrate polypeptide tail being anchored at the scissile residue, these attractions would produce a compressive mechanical force which might suffice to engender a spatial contraction. The shortening of the distances across the individual hydrogen bonds of the chain might then have a multiple effect. The sites could be coupled together,⁴⁹ allowing for charge displacement. The effective pK of the chain might be altered, enhancing its catalytic effect. Finally, in a shortened hydrogen bond, the protons might be unusually mobile, producing isotope effects of 1.5 to 2 at each site.⁵⁰

It will eventually be important to relate the activation of multiproton catalysis to changes in the rate constant, i.e., to establish a connection between increased transition-state stabilization energy, as reflected in a lowered free energy of activation, and the function of the multiproton entity. Some information can be adduced at this point, although enough variation in conditions is present (for example, among the cases cited in Table 7) to make it futile to compare measured values of k_{cat} or k_{cat}/K_m in a simple sense. In the study of Elrod et al.⁷ on trypsin, however, the following comparisons are possible. The minimal substrate Ac-ONp leads to $k_{\text{cat}} \sim 2 \times 10^{-3} \text{ s}^{-1}$ (pH 7.5), and one-proton catalysis. Addition of C_α and *N*-acyl interactions (Bz-Arg) produces $k_{\text{cat}} \sim 7 \text{ s}^{-1}$ (pH 8), a rate increase of 3500-fold (reduction in free energy of activation of 5 kcal/mol), but one-proton catalysis still prevails. Multiproton catalysis enters with the Bz-Phe-Val-Arg substrate ($k_{\text{cat}} \sim 2 \times 10^3 \text{ s}^{-1}$, pH 7.4), accompanied by another 300-fold acceleration, corresponding in free energy to 2.4 kcal/mol.

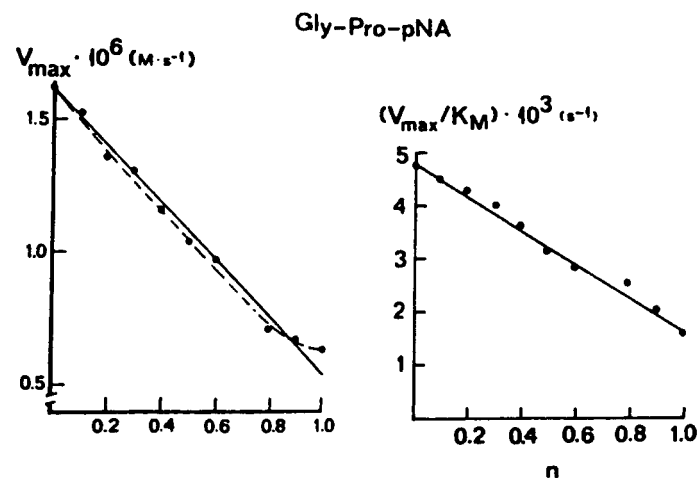
B. Other Serine Hydrolases

1. Dipeptidylpeptidase-IV^{51,52}

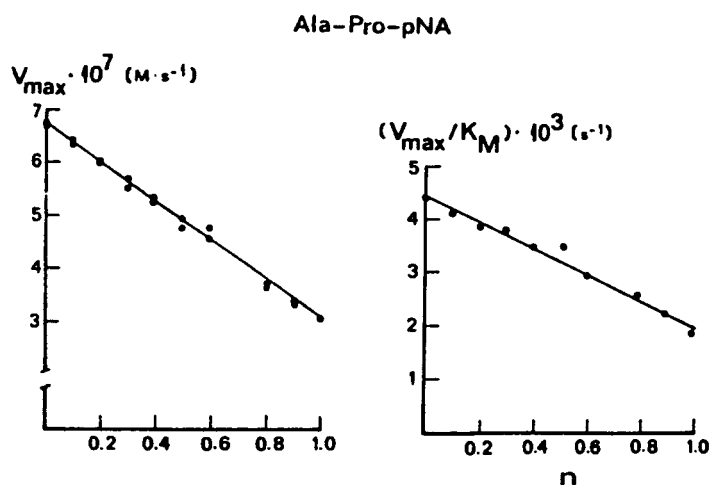
This enzyme specifically cleaves the N-terminal dipeptide from a peptide substrate whenever an Ala or Pro residue is present at the penultimate (thus, scissile) position. Dipeptidylpeptidase-IV (DP-IV) is a serine hydrolase which appears to react by an acylation-deacylation pathway. The high specificity of this enzyme for a terminal dipeptide, together with its character as a serine hydrolase, raises an interesting question of the activation of any charge-relay system which may be present (no crystallographic structure for the enzyme is yet available). As we have seen, the serine-protease data above (limited to endo-proteases) suggest that the long polypeptide tail preceding the scissile residue may be of importance, activating the charge-relay system through its subsite interactions. For a DP-IV there is only a single residue preceding the scissile residue. How, then, does such an enzyme solve the problem of activating its acid-base catalytic machinery?

Careful contributions to the mechanism of DP-IV action, including proton inventories, have been made by A. Barth, G. Fischer, M. Kaiser, and co-workers at the University of Halle-Wittenberg in the German Democratic Republic. We are indebted to these scientists for their generous permission to reproduce their data here. In particular, they have determined the proton inventories for both k_{cat} and k_{cat}/K_m for two substrates, Gly-Pro-NHNp and Ala-Pro-NHNp (Figure 9). For both of these substrates, it is believed that nucleophilic attack to form the tetrahedral adduct determines the rate for k_{cat}/K_m , while hydrolysis of the acyl enzyme is rate-limiting for k_{cat} . The overall isotope effects are similar for k_{cat}/K_m (2.9 for the Gly substrate, 2.4 for the Ala substrate) and for k_{cat} (2.5 and 2.2 for Ala and Gly, respectively). As Figure 9 shows, all proton inventories are linear, corresponding to one-proton catalysis.

The situation is quite different with Ala-Ala-NHNp (Figure 10). Here the rate-limiting process for k_{cat}/K_m has been considered by Barth and co-workers to constitute decomposition



A



B

FIGURE 9. Proton-inventory curves for the action of dipeptidyl-peptidase-IV. (A) Gly-Pro-NHNp. Both curves are linear in the best fit (solid lines) although the v_{\max} data appear visually to be nonlinear (dashed line). (B) Ala-Pro-NHNp. Best fits are linear. These data and figures, courtesy of A. Barth, G. Fischer, and M. Kaiser of the Biosciences Section, University of Halle-Wittenberg, GDR.

of the tetrahedral intermediate. The overall isotope effect is now approximately 2.0 and exhibits clear multiproton character. This line shown is the best-fit curve for two-proton catalysis. The data for K_{cat} , which is also determined by acylation, show a dome shape characteristic of contributions from more than one rate-limiting step or from opposing normal and inverse isotope effects.

Thus, with DP-IV, as with the serine proteases considered above, highly specific enzyme-substrate interactions appear to be required in order to observe multiproton catalysis. The situation may also vary from one mechanistic step to another.

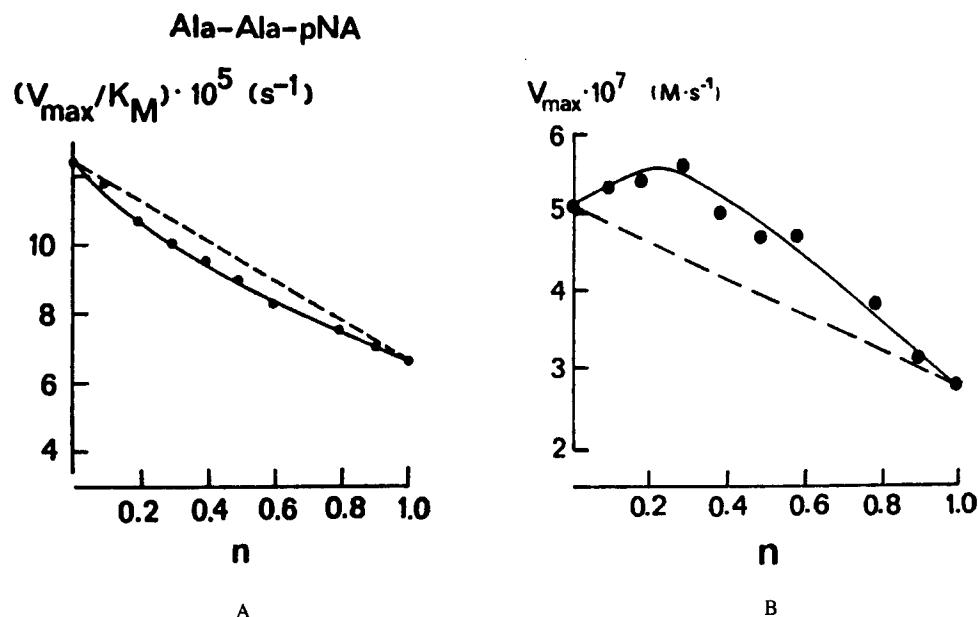


FIGURE 10. Proton-inventory curve for action of DP-IV on Ala-Ala-NHNp. (A) K_{cat}/K_m . The best-fit line is for two-proton catalysis. (B) K_{cat} . The line is for a best-fit polynomial representation. The figure, courtesy of Professor Barth.

2. Amidohydrolases^{8,53}

Proton inventories have been obtained for some reactions catalyzed by amidohydrolases, enzymes which accelerate the hydrolysis of the simple amides, Gln and Asn. Although the crystallographic structures of glutaminases and asparaginases have not been determined, there is enough information available from other approaches to know that their structures are very different from the structures of the serine proteases. The serine proteases are single-subunit enzymes of around 25,000 daltons molecular weight, while a typical asparaginase is a tetrameric aggregate with a molecular weight around $4 \times 35,000$ daltons. Nevertheless, there is substantial mechanistic affinity between the two kinds of enzymes. It appears that the amidohydrolases are, in fact, serine hydrolases, employing a typical double-displacement mechanism.

The enzymes occur in many organisms, but the ones for which results are given here are of bacterial origin. The specificity pattern varies with the source of the enzyme, but the typical picture is for fairly rigid specificity. Nearly always the α -carboxylate is required, although the α -ammonio group may be dispensed with, usually at considerable cost in activity.

Commonly, the specificity is much higher for the parameter k_{cat}/K_m than it is for k_{cat} . For example, the asparaginase of *Erwinia carotovora* exhibits a 6000-fold reduction in k_{cat}/K_m when the α -ammonio group of Asn is omitted (to give succinamic acid), but k_{cat} is reduced only fourfold.

Table 8 shows some results obtained for asparaginases and for a single glutaminase, that of *Escherichia coli*. Instead of using the graphical method of examining these proton inventories, we use a different method: *midpoint solvent isotope effects*. For the three simplest models of proton inventories (Table 1: one-proton, two-proton, and many-proton catalysis), the maximum dispersion between the predicted curves occurs at the "midpoint" of the isotopic solvent mixture, $n = 0.5$. If one has a measurement at or near this value, one may simply compare the observation for this point with the prediction from the three models. The requisite formulas for $n = n_m$, a value near 0.5, are readily obtained from Table 1:

Table 8
COMPARISON OF OBSERVED MIDPOINT PARTIAL SOLVENT ISOTOPE
EFFECTS WITH PREDICTIONS FOR VARIOUS MECHANISTIC MODELS

Enzyme and substrate* (average range of data, ppt); overall effect, V_o/V_i	Obsd. V_m/V_i (n_m)	Predicted V_m/V_i (deviation from obsd, ppt)		
		One-proton catalysis	Two-proton catalysis	Many-proton catalysis
<i>Escherichia</i> asparaginase, asparagine (± 14); 2.93	1.720(0.495)	1.935(+125)	1.816(+56)	1.697(-13)
<i>Erwinia</i> asparaginase, asparagine (± 17); 2.62	1.716(0.491)	1.828(+65)	1.731(+9)	1.635(-47)
<i>Proteus</i> asparaginase, asparagine (± 9); 3.31	1.913(0.497)	2.158(+128)	1.990(+40)	1.824(-47)
<i>Escherichia</i> glutaminase, glutamine (± 27); 1.80	1.352(0.495)	1.401(+36)	1.373(+16)	1.343(-7)
<i>Erwinia</i> asparaginase, glutamine (± 23); 1.90	1.522(0.488)	1.468(-35)	1.431(-60)	1.394(-84)
<i>Escherichia</i> asparaginase, glutamine (± 10); 1.69	1.368(0.467)	1.354(-10)	1.332(-26)	1.312(-41)

$$\text{one-proton catalysis: } v_m/v_i = (1 - n_m)(v_o/v_i) + n_m$$

$$\text{two-proton catalysis: } v_m/v_i = \{(1 - n_m)(v_o/v_i)^{1/2} + n_m\}^2$$

$$\text{many-proton catalysis: } v_m/v_i = (v_o/v_i)^{(1 - n_m)}$$

The data for the proton inventories described in Table 8 were all obtained at single substrate concentrations 20- to 100-fold larger than the corresponding K_m value so that the weighting factor for k_{cat} in the observed isotope effects is 0.95 to 0.99. The effects can, thus, be considered as essentially k_{cat} effects.

The table shows, in addition to the predicted midpoint solvent isotope effects, the magnitude of the overall solvent isotope effect for each system, the observed midpoint effects, and the average range for a single point in the individual data sets. For each prediction, its deviation from the observed value in parts per thousand is tabulated. By comparing these with the average range for an individual point, in parts per thousand, one gets an idea of which model fits best and how reliable the conclusion is.

The first four entries of Table 8 are for the evolutionarily anticipated combinations of enzymes and substrates: asparaginases with Asn and glutaminases with Gln. For the first three cases, the one-proton prediction is much above the observation: by 9-fold, 4-fold, and 14-fold the average range of a data point, respectively. This seems to exclude one-proton catalysis quite reliably. For the fourth case, the prediction exceeds the range by only 50%, but if one considers that the *range* of the data, not the standard deviation, is being employed, the rejection of one-proton catalysis seems quite conclusive here, too.

For all four cases, the observed effects lie between the predictions for two-proton catalysis and many-proton catalysis. This suggests that, for specific substrates, some kind of multi-proton catalysis is at work, although the number of protons involved is not necessarily two, and may well be greater.

For the last two cases in the table, the substrate is not evolutionarily adapted to the enzyme: in both cases, glutamine is the substrate for an asparaginase. Here, all predictions lie below the observations. For Gln with *Escherichia* asparaginase, the deviation from the linear prediction is not impressive, and, statistically, this curve may be regarded as conforming to one-proton catalysis. The observations for *Erwinia* asparaginase, on the other hand, lie

farther above the linear prediction. This is the sign of a dome-shaped proton-inventory curve. The mechanistic basis for the dome-shape proton inventory is not known, because the data can be equally fit by any of the possible models. For example, the data, which give an overall solvent isotope effect of 1.90, can be described by:

$$v_n/v_1 = (1.90)[1 - n + n/(2.4)](1 - n + 1.25n)$$

which corresponds to a transition state with a one-proton catalytic bridge ($k_H/k_D = 2.4$) and one site at the hydroxyl group of a tetrahedral adduct ($\phi = 1.25$). It is conceivable that such a transition state might arise here. Also, however, the same line describes the curve,

$$v_n/v_1 = (1.90)\{0.45 + [0.55/(1 - n + n/[2.6])]\}^{-1}$$

which corresponds to two steps, each partly determining the rate in HOH. One step (weighting factor 0.45) gives no isotope effect and might be a "physical step" such as product release. The other (weighting factor 0.55) gives a one-proton isotope effect of 2.6 and might be the ordinary sort of one-proton catalysis seen with nonspecific substrates for the serine proteases. The choices of weighting factors and isotope effects are, of course, arbitrary and serve only to illustrate a possible fit to the data; other support would be required to base a mechanistic hypothesis on the concept of dual rate-limiting steps for Gln.

These data do appear to coincide with those for the serine proteases in one important way. Specific substrates give multiproton catalysis; nonspecific substrates give either one-proton catalysis or a dome-shaped proton inventory of still unknown origin, but which may arise from more than one rate-limiting step.

More detailed studies are available for a single example of a nonspecific substrate, succinamic acid with *Erwinia* asparaginase. Succinamic acid corresponds, in effect, to the natural substrate Asn but with the α -ammonio functional group removed. The proton inventories for k_{cat} and for k_{cat}/K_m were obtained by application of the weighting-factor method in seven isotopic solvent mixtures.⁵³ The results are shown in Figure 11.

The overall isotope effect on k_{cat} is 2.22 and, as the figure shows, the proton inventory indicates more than a single site. The square-root plot, although not shown, is linear. The data, thus, support the idea that two-proton catalysis, observed with the natural substrate Asn with an overall isotope effect of 2.6, continues to be seen upon omission of an important structural feature, the α -ammonio group. If, as in the serine proteases, the detailed interaction of substrate features with the enzyme in the catalytic transition state enables the function of some multiproton catalytic entity, then it is not wholly disabled by the loss of the α -ammonio interaction. This is further consistent with the fact that the value of k_{cat} is only slightly reduced by this omission (fourfold).

The overall effect on k_{cat}/K_m is much smaller (1.4), and although the plot is visually linear, it is not easy at this magnitude of overall effect to distinguish reliably between one-proton and two-proton catalysis. At this point, we also lack a proton inventory for k_{cat}/K_m for the natural substrate Asn. The comparison between these results and the data for Asn, when they are obtained, will be of great interest, because there is a large rate effect of structure on this kinetic term. The loss of the α -ammonio group reduces k_{cat}/K_m by a factor of 6000.

To date, then, the picture for the amidohydrolases is not inconsistent with that for other serine hydrolases: a multiproton catalytic entity which seems to be activated by structural interaction between enzyme and evolutionarily anticipated ("natural") substrate features in the catalytic transition state. Sufficient alteration of these features (extension of the structure by one methylene group to give Gln) disables the multiproton entity, although other structural alterations may not have so severe an effect (as in succinamate anion).

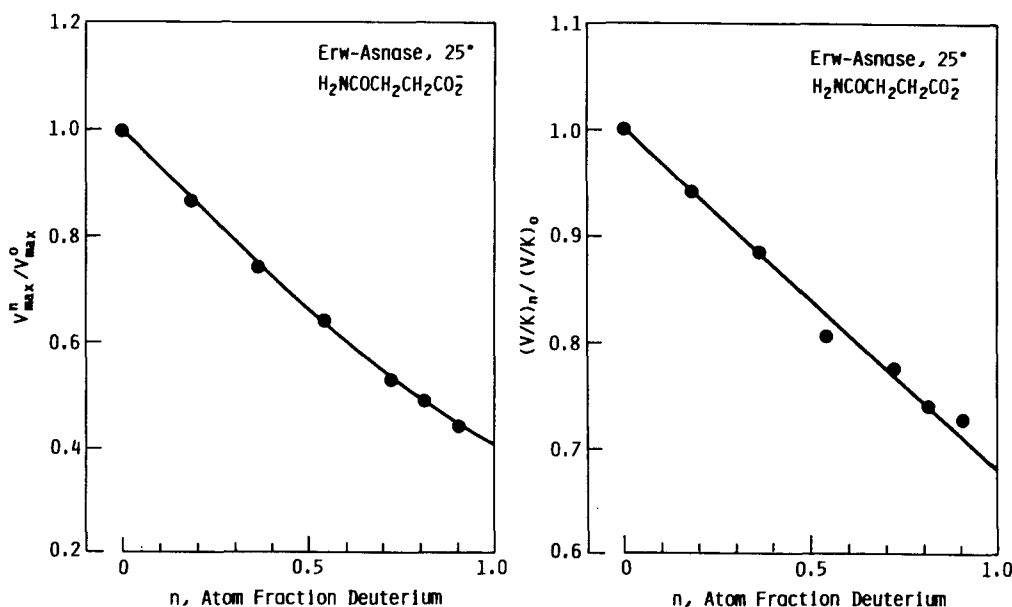


FIGURE 11. Proton-inventory curves for the action of the asparaginase of *Erwinia carotovora* on succinate anion.

3. Acetylcholinesterase⁵⁴

This serine hydrolase is of far greater structural complexity than the serine proteases, but enjoys the double-displacement mechanism. Its natural substrate is the simple ester acetylcholine, $\text{CH}_3\text{COOCH}_2\text{CH}_2\text{N}(\text{CH}_3)_3^+$, so that the question of remote subsites is removed (although there clearly is a cation-binding site for the ammonio group). Acetylcholine itself shows no solvent isotope effect⁵⁵ and probably has some physical event in the course of binding to the enzyme as the rate-determining process in k_{cat}/K_m . Ac-ONp has a value of k_{cat}/K_m reduced 1000-fold from that of acetylcholine, and exhibits a solvent isotope effect of about 1.6. Although such an effect is at the borderline of interpretability because of its small magnitude, some quite precise measurements and the shape of the proton-inventory curve (Figure 12) save the day.

The curve is dome-shaped and, thus, consistent most straightforwardly with models involving either contributions from both inverse and normal isotope effects (this was the originally favored interpretation⁵⁴) or with a change in rate-determining step. The latter interpretation now appears favorable when one recognizes that the chemical "steps" in which acid-base catalysis should occur, and in which isotope effects will, therefore, appear, may be coming into view with this relatively poor substrate. In fact, the data of Figure 12 can be fit adequately to this arbitrarily chosen model equation for two transition states in series:

$$(k_{\text{cat}}/K_m)_n / (k_{\text{cat}}/K_m)_1 = (1.56)\{0.44 + [0.56/(1 - n + n/2)]\}^{-1}$$

This corresponds to a "physical step" (weight 0.44) and a "chemical step" (weight 0.56) having a reasonable one-proton isotope effect of 2.

C. Papain, a Cysteine Protease⁵⁶

Papain is a cysteine protease, a member of the class of enzymes closely related in structure

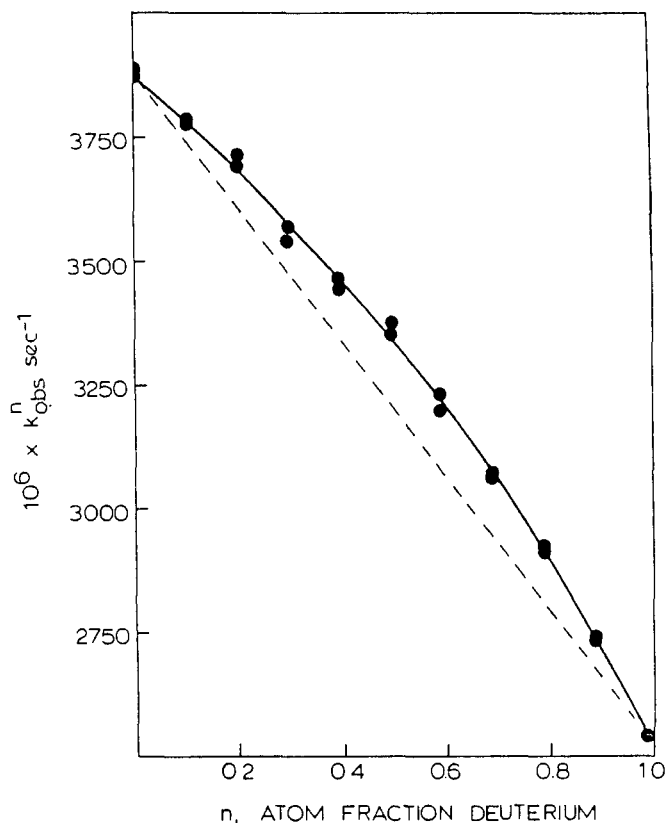


FIGURE 12. Proton-inventory curve for the acetylation of acetylcholinesterase by Ac-ONp. (Reprinted with permission from Hogg, J. L., Elrod, J. P., and Schowen, R. L., Transition-state properties and rate-limiting processes in the acetylation of acetylcholine by natural and unnatural substrates, *J. Am. Chem. Soc.*, 102, 2082, 1980. Copyright 1980, American Chemical Society.)

and function to the serine proteases but which differ in having a cysteine residue in place of the serine and, thus, a sulfhydryl nucleophile in place of a hydroxyl nucleophile. Many features, including the double-displacement mechanism, the structural potential for charge-relay catalysis, and the presence of subsites for interaction with the polypeptide tail of the substrate, are shared with the serine proteases.

Szawelski and Wharton⁵⁶ have published a very thorough account of the proton-inventory results for the deacylation reaction with three substrates: Cbz-Gly-ONp, Cbz-Lys-ONp, and MeOCO-Phe-Gly-ONp. The series, therefore, bears a strong relationship to the series of studies with the serine proteases. A typical result is shown in Figure 13. For these *p*-nitrophenyl esters, the deacylation step is rate determining, so that the reactant state may be considered to a first approximation not to have unusual fractionation factors (the reactant state being a thiol ester of the enzyme, the sulfhydryl group is not present to complicate matters).

The results are quite similar for all three substrates. As is clear from the figure, the proton inventory curve is essentially linear. In fact, when Szawelski and Wharton deliberately fit the data to a two-proton model (an excellent approach to checking for the validity of the one-proton model), the second fractionation factor was calculated as 1.01 to 1.09, showing

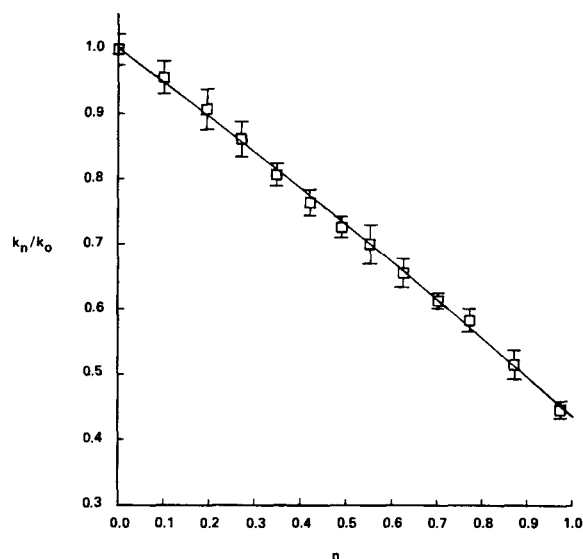


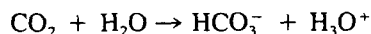
FIGURE 13. Proton-inventory curve for the action of papain on Cbz-Lys-ONp. (From Szawelski, R. J. and Wharton, C. W., *Biochem. J.*, 199, 681, 1981. With permission.)

the strong consistency of the data for all substrates with a one-proton model (the slightly curved line in Figure 13 is calculated from such a fit). Thus, the isotope effects of 2.2 to 2.3 apparently arise from one transition-state site. Szawelski and Wharton ascribe this to the bridging site between the active-site His imidazole and the oxygen of a water molecule attacking the thiol-ester carbonyl group. From a theoretical analysis, they conclude that the proton is participating in the reaction-coordinate motion. Since this motion also involves the heavy atoms, the magnitude of the isotope effect is not large, but only 2 to 2.5.

Szawelski and Wharton note that the use of more extended substrates might lead to charge-relay catalysis here as in the serine proteases, although they recognize that the structural evidence concerning both serine and cysteine proteases, which refers to reactant states, precludes charge-relay function in these states. The paper of these two authors is especially valuable, not only for its accurate and extensive data and its thoughtful interpretation, but also for the unusually careful and rigorous statistical treatment of the proton-inventory results.

D. Carbonic Anhydrase^{9,57}

The progression in this series of case studies of proton-inventory applications to enzymology has included enzymes with quite large substrates (polypeptides) as well as those with smaller substrates such as dipeptides and acetylcholinesterase. Now we reach the terminus of this progression with carbonic anhydrase (CA), which has as its substrate the triatomic molecule carbon dioxide:



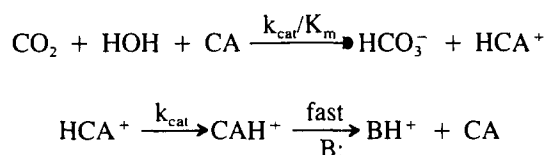
CA is also of interest as a metalloenzyme, an active-site Zn^{2+} being important in catalysis.

Silverman and co-workers Venkatasubban and Tu have determined proton inventories on the individual kinetic parameters for the steady-state hydration reaction⁹ catalyzed by bovine red-cell CA, and for an informative isotope-exchange reaction⁵⁷ catalyzed by human CA.

One of their results has been presented already in the introductory section. Figure 1C shows the proton inventory curve for k_{cat} for the hydration of CO_2 catalyzed by CA of bovine

red blood cells. A similar semilogarithmic plot for K_m is equally linear. The overall solvent isotope effects are 3.24 ± 0.37 (k_{cat}) and 3.00 ± 0.35 (K_m), so that the kinetic parameter k_{cat}/K_m must display only a small overall isotope effect (1.08 ± 0.25). Since the semilogarithmic plots are linear, both proton inventories are accurately described by an exponential function. The rate-determining step for k_{cat}/K_m has only a very small solvent isotope effect and probably involves no component of protonic reorganization, while the k_{cat} isotope effect arises from a number of sites.

Venkatasubban and Silverman interpreted this result in terms of the mechanism:

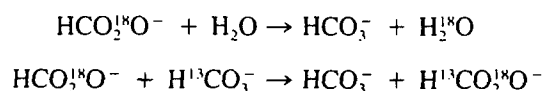


Here the rate of overall conversion of CO_2 to HCO_3^- is given by k_{cat}/K_m , which has no isotope effect. It was, therefore, concluded that the rate-limiting step in this part of the reaction involved no protonic reorganization. One possible candidate is a "physical step", such as the binding of reactant or the release of the product.

The k_{cat} process is assumed to be the "shuttle" of a proton from its final point in the preceding reaction stage to another group more accessible to the aqueous solvent. From this group, the proton is then removed, in a step which is known to be rapid, by the buffer base. The "shuttle" might have been a simple proton-transfer reaction between the two groups. Then, however, the isotope effect would have originated in a single site. The proton inventory would have been linear, while, in fact, it is exponential. Venkatasubban and Silverman have, therefore, favored the alternative view that the transfer occurs across intervening water molecules, so that several sites (they suspect three) are producing simultaneous isotope effects. Such a three-proton model produces fair agreement with the observations.

Another possibility is that an even larger number of protons, involved, for example, in a protein conformational change, produce the exponential proton inventory. Such a conformational change might precede the "shuttle" of the proton, perhaps bringing the participating groups and intervening water molecules into favorable alignment for motion of the proton in a fast step. Silverman and Tu have discussed the probable role of such a conformational change in a different context.⁵⁷

With human CA, the same group has studied two isotope exchange reactions catalyzed by the enzyme.⁵⁷ These are



Analysis of the biexponential kinetics exhibited by each of these processes allows calculation of two interesting rates:

- R_1 : the rate of conversion of HCO_3^- to CO_2
- R_{HOH} : the rate of release of water which bears substrate oxygen from its zinc-bound form on the enzyme

Abbreviated but highly informative proton-inventory data have been obtained for each of these (rates at $n = 0.00, 0.49$, and 0.98). The rate R_1 shows no isotope effect at all. This

is wholly consistent with the observation that the steady-state parameter, k_{cat}/K_m , also representing conversion of CO_2 to HCO_3^- , did not display a solvent isotope effect.

The R_{HOH} processes exhibited a very large solvent isotope effect of 8.0 ± 0.7 . The data at $n = 0.49$ are approximately consistent with an exponential proton inventory as this calculation shows:

$$R_{\text{HOH}}/R_{\text{DOD}} = 8.0$$

$$(R_{\text{HOH}}/R_{\text{DOD}})^{0.51} = 2.89 \quad (\text{expected midpoint solvent isotope effect at } n = 0.49 \text{ for many-proton catalysis})$$

$$R_{\text{LOL}}^{n=0.49}/R_{\text{DOD}} = 2.7$$

The R_{HOH} process, thus, displays the same *type* of proton inventory (many-proton) as was observed in the steady state for k_{cat} . This makes excellent sense, since the mechanistic hypothesis was that the proton shuttle determined the rate there. Very likely, the event that permits the substrate oxygen (bound as hydroxyl to the active-site zinc) to be lost into the water is the conversion to a labile water molecule through shuttle of a proton to the oxygen. This could be the same shuttle reaction under observation in the steady state, or a similar one.

The *magnitude* of the isotope effect for R_{HOH} is much greater than for k_{cat} (8.0 vs. 3.2). Could it be that the proton shuttle has an intrinsic isotope effect of 8, and that another step (say, a physical step) intervenes and partially determines the rate in the steady-state reaction, this diluting the isotope effect to 3.2? This was excluded by Venkatasubban and Silverman because the shape of the proton-inventory curve is wrong: a change in rate-limiting step will drive the curve toward a dome shape. A statistical comparison of the models tends to confirm the conclusion. The observed magnitude of 3.2 for the overall steady-state solvent isotope effect would require weighting factors of 0.67 for the physical step ($k_{\text{H}}/k_{\text{D}} = 1$) and 0.33 for the proton-shuttle step ($k_{\text{H}}/k_{\text{D}} = 8$). The resulting proton-inventory equation would therefore be

$$(k_{\text{cat}}^n/k_{\text{cat}}^1) = 3.2/[0.67 + 0.33(8.0)^n]$$

The fit of this equation to the data is much worse than the simple exponential fit. The simple exponential proton inventory accounts for 99.7% of the variation in the data, and the model above for only 93.3%. This explanation of the difference in isotope effects does not seem to be correct, therefore, and the true reason remains unknown.

E. Phosphatases

1. Inorganic Pyrophosphatase⁵⁸

This Mg^{2+} -requiring enzyme catalyzes the hydrolysis of the anhydride linkage of pyrophosphate anion to yield two phosphate anions. Konsowitz and Cooperman⁵⁸ measured the proton inventory data shown in Figure 14. Rate measurements were made at the rate-maximum of the bell-shaped pL/rate profile in each isotopic solvent (from pH 7.0 in HOH to pD 7.5 in DOD). The overall isotope effect was 1.45 ± 0.05 .

The result is a dome-shaped curve, with two simple interpretations: conflicting inverse and normal effects, *or* change in rate-determining step. Reasoning that the reactant Mg^{2+} would have a coordinated water molecule, $[\text{Mg} \cdots \text{OH}_2]^+$, Konsowitz and Cooperman recognized that displacement of this water could provide an inverse isotope effect (ϕ for each of the two protonic sites of coordinated water should be between 0.69 and unity, so that displacement into bulk solution would give an inverse isotope effect $k_{\text{D}}/k_{\text{H}} = 1$ to

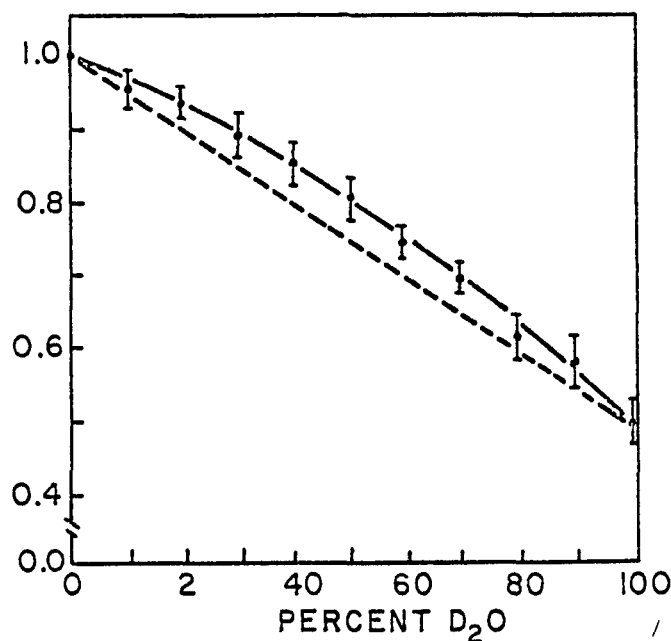
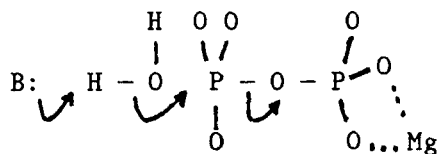


FIGURE 14. Proton-inventory curve for the action of inorganic pyrophosphatase on pyrophosphate anion, with Mg^{2+} as cofactor. (From Kon-sowitz, L. M. and Cooperman, B. S., Solvent isotope effect in organic pyrophosphatase-catalyzed hydrolysis of inorganic pyrophosphate, *J. Am. Chem. Soc.*, 98, 1993, 1976. With permission. Copyright 1976, American Chemical Society.)

1.45). They chose $\phi_1^R = \phi_2^R = 0.90$ as possible values and obtained the proton-inventory curve,

$$(k_n/k_o) = (1 - n + n/2.5)/[1 - n + n(0.90)]^2$$

by fitting to the data. This curve is shown in the figure. The transition-state isotope effect of 2.5 could come from general-base catalysis:



Several other models were also considered.

Later work by Cooperman and collaborators⁵⁹ has shown that a change in rate-limiting step is the more likely explanation. Using a combination of steady-state rate measurements, equilibrium measurements, and isotope-exchange studies, they found from calculation of microscopic rate constants for pyrophosphatase action that product-release, rather than fission of the anhydride linkage, was a major determinant of both the isotope effect and the rate when the natural cofactor Mg^{2+} was used. When other metal ions were substituted, product-release became slower and the solvent isotope effect increased. The slower product-release

accounted for the lower rates with other metal ions. The relative rates and overall solvent isotope effects were Mg^{2+} (1.00, 1.75); Zn^{2+} (0.26, 2.56); Co^{2+} (0.08, 2.22); Mn^{2+} (0.09, 2.86).

If we arbitrarily assume, on the basis of the Mn^{2+} result, that the solvent isotope effect for product release is 3, and the other steps determining the rate for the Mg^{2+} case have no solvent isotope effect, then we obtain the following weighting factors:

Step	Weighting factor	Solvent isotope effect
Product-release	0.5	3
Other steps	0.5	1

We can consider two models for the product-release step: (1) a protein conformation change precipitated by a single-site event such as a proton transfer; (2) a protein conformational change involving many sites, as in hydrogen bonding and solvation changes. Predicted proton inventories for each of these can be fitted to the data and the fits compared with each other:

Model	Predicted proton inventory	Percent of variation fit
One site	$k_n/k_o = \{0.5 + [0.5/(1 - n + n/3)]\}^{-1}$	99.6
Many sites	$k_n/k_o = [0.5 + 0.5(3^n)]^{-1}$	93.0

Thus, the one-site model for the solvent isotope effect on product release clearly fits the data far better than the many-site model. In fact, the one-site curve is essentially superimposable on the curve shown in Figure 14, while the many-site curve lies fairly far below the points (less dome-shaped). The reason is that the exponential character of the isotope effect, in the many-site model, a contribution that tends toward a bowl shape, cancels the dome-shaped tendency arising from the shift in the rate-limiting step. This produces a nearly linear curve.

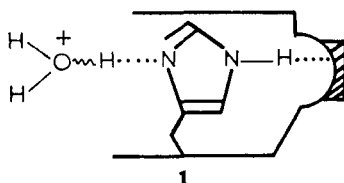
It may seem a peculiar suggestion that a single-proton event like proton transfer might initiate a large-scale structural change such as the conformational alteration involved in product release. However, it may well be that the catalytic structure of the enzyme is maintained by an interaction which is destroyed when a proton is transferred. An electrostatic "salt bridge" is a simple candidate. Such a suggestion has previously been made for a conformational change of ribonuclease, discussed in the next section.

2. Ribonuclease⁶⁰

Ribonuclease undergoes a conformation change, perhaps an event in the binding of substrate, which (because a hydrogen ion is released) can be observed by indicator methods in temperature-jump experiments. The proton-inventory curve for this process, which has an overall solvent isotope effect of 4.8, is bowl-shaped, suggesting a multisite effect. The model which was originally fit to the data was

$$k_n/k_o = (1 - n + n/2.2)(1 - n + 0.69n)^2$$

This model was felt to arise from this transition-state structure:



where a proton transfer is occurring from a histidine imidazolium to an adjacent water molecule. Such a proton transfer might very well have a transition state strongly resembling the hydronium ion (the reaction being energetically "uphill"), with a fractionation factor of 0.69 for the two sites attached to positive oxygen (Table 3) and an isotope effect of 2.2 from the "in-flight" proton which is very asymmetrically located. The transfer of the proton neutralizes the imidazole, breaking a "salt bridge" and triggering the conformational change.

The proposal is imaginative and still exerts a charm on the one of us involved in it originally. It is necessary to admit, however, that an exponential fit to the data is essentially as good as the fit of the model suggested above. To distinguish a "medium effect" model from the proton-transfer (three-site) model will, therefore, require other evidence.

F. Two Cases Involving Macromolecular Association

Proton inventories might be expected to be particularly informative about reactions in which macromolecules of biological interest undergo association or dissociation, since such processes have long been thought to be affected by DOD. One case, subunit association of formyltetrahydrofolate synthetase, has been discussed in previous reviews.^{2,4} It will be considered only briefly here.

1. Formyltetrahydrofolate Synthetase⁶¹

Some years ago, Harmony and co-workers examined the kinetics and thermodynamics of association of this tetrameric enzyme from its free subunits.⁶¹ The subunits are stabilized in the tetrameric aggregate, which is the only enzymically active form, by two monovalent cations (K^+ or Tl^+ in these studies). The equilibrium constant for combination of four monomeric subunits and two cations to give the active tetramer is some 60-fold larger in DOD than in HOH. The rate of tetramer formation, which is second order in monomer and first order in cation, is around 2.8-fold faster in DOD. Struck by the fact that $2.8^4 = 60$, the investigators plotted $K_n^{1/4}$ vs. n (where K_n is the equilibrium constant for tetramer formation). They found the plot to be excellently linear. The data are, therefore, consistent with the following model:

1. In the mechanism of tetramerization, there is an initial fast binding of a cation to a monomer ($K_D/K_H = 2.8$), with the overall rate-determining step being diffusion of this complex toward free monomer: thus, the kinetic isotope effect is $k_D/k_H = 2.8$.
2. The rapid remainder of the tetramerization reaction consists of several steps, the first being completion of complex formation of the two monomers with the single cation. As the cation enters the binding site of the second monomer, another solvent isotope effect of 2.8 is produced. This entire process is repeated independently (with an isotope effect here also of $[2.8]^2$). Then, in the final state, the two dimer-cation complexes combine with no solvent isotope effect to give the active tetramer. Thus, equilibrium formation of tetramer has $K_D/K_H = (2.8)^4 = 60$.

The detailed physical origin of the isotope effect from insertion of the cation into its binding site on each of the monomers remains unknown. The greatest value of the work, however, is that it demonstrates that the very large isotope effects on protein association may, in fact, arise from a rather small number of reasonably ordinary isotope effects at individual sites.

2. Valyl-tRNA Synthetase⁶²

This enzyme catalyzes the aminoacylation of $tRNA^{Val}$ to form Valyl $tRNA^{Val}$ in a two-stage reaction.⁶³ First, the enzyme binds the amino acid and ATP and catalyzes the displacement of pyrophosphate by the amino-acid carboxylate center. The result is an aminoacyladenylate, an activated carboxylic-phosphoric anhydride. Then the enzyme binds the

tRNA and catalyzes the displacement of AMP from the anhydride by the 3' hydroxyl of a tRNA terminal residue, to generate the aminoacyl tRNA (Valyl-tRNA^{Val}). This later participates in protein biosynthesis. The yeast enzyme, for which extensive solvent isotope effect work has been carried out by Kern et al.,⁶² is a monomeric enzyme of molecular weight 122 kilodaltons. It has a single binding site for each of Val, tRNA^{Val}, and ATP.

The most striking point to notice initially in the work of these authors is the number of processes which exhibit *no solvent isotope effect at all* (at least for pH = pD):

1. The thermal stability of the synthetase
2. The association of the synthetase with tRNA^{Val}, measured either from Scatchard plots or from the K_m values in the aminoacylation reaction kinetics
3. The K_m values for Val and ATP
4. The rate of the pyrophosphate/ATP isotope (³²P) exchange

This is quite striking and makes the point very strongly that there need not be large solvent isotope effects, nor, indeed, any effect at all, associated with processes that involve extremely extensive macromolecular interaction.

The k_{cat} value for the aminoacylation reaction does exhibit a solvent isotope effect. The overall effect is between 5 and 6. The proton inventory is quite linear and implies, therefore, that this effect arises from a single site. As the authors point out, this excludes the intimate participation of a sulfhydryl group, which would have an initial-state fractionation factor of about 0.4. If the proton were transferred in the transition state, the resulting combination of inverse and normal contributions to the isotope effect would have conferred a dome shape on the proton inventory. In fact, the large, one-site isotope effect, together with an apparent temperature independence of the solvent isotope effect (reminiscent of a similar observation for trypsin⁶⁴) raises the question whether proton tunneling may not be important in this reaction.

IV. SUMMARY AND PROSPECTS

These examples of the proton inventory technique have illustrated some of its potential for extending the understanding of enzyme mechanisms. In some simple cases, a literal proton inventory has been possible. In other cases, indications of more complex mechanistic phenomena, such as changes in rate-limiting step, have emerged. As experience continues to accumulate, confidence will grow in the interpretation of typical observations. To some extent, future increases in experimental precision may help to define more exactly the shape of proton-inventory curves and to narrow the range of models that fit a given set of observations. In all cases, the emphasis will continue to fall on proton inventories as components of a general study of reaction mechanism, contributing along with other probes to the development of acceptable mechanistic pictures.

REFERENCES

1. Melander, L. and Saunders, W. H., Jr., *Reaction Rates of Isotopic Molecules*, Wiley-Interscience, New York, 1980, chap. 7.
2. Schowen, K. B. and Schowen, R. L., Solvent isotope effects on enzyme systems, *Methods Enzymol.*, 87C, 551, 1982.
3. Schowen, K. B., Solvent hydrogen isotope effects, in *Transition States of Biochemical Processes*, Gandour, R. D. and Schowen, R. L., Eds., Plenum Press, New York, 1978.

4. Schowen, R. L., Solvent isotope effects on enzymic reactions, in *Isotope Effects on Enzyme-Catalyzed Reactions*, Cleland, W. W., O'Leary, M. H., and Northrop, D. B., Eds., University Park Press, Baltimore, 1977, 64.
5. Gold, V., Protolytic processes in H₂O-D₂O mixtures, *Adv. Phys. Org. Chem.*, 7, 259, 1969.
6. Kresge, A. J., Solvent isotope effects in H₂O-D₂O mixtures, *Pure Appl. Chem.*, 8, 243, 1964.
7. Elrod, J. P., Hogg, J. L., Quinn, D. M., and Schowen, R. L., Protonic reorganization and substrate structure in catalysis by serine proteases, *J. Am. Chem. Soc.*, 102, 3917, 1980.
8. Quinn, D. M., Venkatasubban, K. S., Kise, M., and Schowen, R. L., Protonic reorganization and substrate structure in catalysis by amidohydrolases, *J. Am. Chem. Soc.*, 102, 5365, 1980.
9. Venkatasubban, K. S. and Silverman, D. N., CO₂ hydration activity of carbonic anhydrase in mixtures of H₂O and D₂O, *Biochemistry*, 19, 4984, 1980; Silverman, D. N. and Vincent, S. H., Proton transfer in the catalytic mechanism of carbonic anhydrase, *CRC Crit. Rev. Biochem.*, 14, 207, 1983.
10. Kresge, A. J., Solvent isotope effects and the mechanism of chymotrypsin action, *J. Am. Chem. Soc.*, 95, 3065, 1973.
11. Albery, W. J., Solvent isotope effects, in *Proton-Transfer Reactions*, Caldin, E. and Gold, V., Eds., Chapman and Hall, London, 1975, 263.
12. Pollock, E., Hogg, J. L., and Schowen, R. L., One-proton catalysis in the deacetylation of acetyl- α -chymotrypsin, *J. Am. Chem. Soc.*, 95, 968, 1973.
13. Urey, H. C., Brickwedde, F. G., and Murphy, G. M., A hydrogen isotope of mass. II, *Phys. Rev.*, 39, 164, 1932.
14. Brickwedde, F. G., Harold Urey and the discovery of deuterium, *Phys. Today*, 35(9), 34, 1982.
15. Calvin, M., G. N. Lewis, *Proc. of the Robert A. Welch Foundation Conf. Chemical Research*, XX, Milligan, W. O., Ed., American Chemistry-Bicentennial, Houston, Tex., 1977, chap. 8.
16. Gross, Ph., Steiner, H., and Krauss, F., On the decomposition of diazoacetic ester catalyzed by protons and deuterons, *Trans. Faraday Soc.*, 32, 877, 1936.
17. Gross, Ph. and Wischin, A., On the distribution of picric acid between benzene and mixtures of light and heavy water, *Trans. Faraday Soc.*, 32, 879, 1936.
18. Gross, Ph., Steiner, H., and Suess, H., The inversion of cane sugar in mixtures of light and heavy water, *Trans. Faraday Soc.*, 32, 883, 1936.
19. Schwartzenbach, G., Dissoziationskonstanten des schweren Wassers und der in ihm gelösten Elektrolyte, *Z. Elektrochem.*, 44, 46, 1938.
20. Gross, Ph., Über Dissoziationskonstanten von Säuren in Mischungen aus leichtem und schwerem Wasser, *Z. Elektrochem.*, 44, 299, 1938.
21. Bigeleisen, J., Statistical mechanics of isotopic systems with small quantum corrections. I. General considerations and the rule of the geometric mean, *J. Chem. Phys.*, 23, 2264, 1955.
22. Orr, W. J. C. and Butler, J. A. V., The kinetic and thermodynamic activity of protons and deuterons in water-deuterium oxide mixtures, *J. Chem. Soc.*, p. 330, 1937.
23. Barnes, T. C. and Larson, E. J., Influence of heavy water of low concentration on *Spirogyra*, *Planaria*, and an enzyme system, *Protoplasma*, 22, 431, 1934.
24. Barbour, H. G. and Dickerson, V. C., The pharmacological action of deuterium oxide. VII. Its effect on the hydrolysis of acetylcholine, *J. Pharmacol. Exp. Ther.*, 65, 281, 1939.
25. Bell, R. P., *The Proton in Chemistry*, Cornell University Press, Ithaca, 1959.
26. Melander, L., *Isotope Effects on Reaction Rates*, Ronald Press, New York, 1960.
27. Purlee, E. L., On the solvent isotope effect of deuterium in aqueous acid solutions, *J. Am. Chem. Soc.*, 81, 263, 1959.
28. Hopper, C. R., Schowen, R. L., Venkatasubban, K. S., and Jayaraman, H., Proton inventories of transition states for solvation catalysis and proton-transfer catalysis. Decomposition of the tetrahedral intermediate in amide methanolysis, *J. Am. Chem. Soc.*, 95, 3280, 1973.
29. Stein, R. L., Analysis of kinetic isotope effects on complex reactions utilizing the concept of the virtual transition state, *J. Org. Chem.*, 46, 3328, 1981.
30. Northrop, D. B., Determining the absolute magnitude of hydrogen isotope effects, in *Isotope Effects on Enzyme-Catalyzed Reactions*, Cleland, W. W., O'Leary, M. H., and Northrop, D. B., Eds., University Park Press, Baltimore, 1977.
31. Gandour, R. D., Coyne, M., Stella, V. J., and Schowen, R. L., Proton inventory of phthalic anhydride hydrolysis. Comments on analysis of proton-inventory data, *J. Org. Chem.*, 45, 1733, 1980.
32. Fersht, A., *Enzyme Structure and Mechanism*, Freeman, San Francisco, 1977.
33. Walsh, C., *Enzymatic Reaction Mechanisms*, Freeman, San Francisco, 1979.
34. Hegazi, F., Quinn, D. M., and Schowen, R. L., *Transition States of Biochemical Processes*, Gandour, R. D. and Schowen, R. L., Eds., Plenum Press, New York, 1978, chap. 10.
35. Blow, D. M., Birktoft, J. J., and Hartley, B. S., Role of a buried acid group in the mechanism of action of chymotrypsin, *Nature (London)*, 221, 337, 1969.

36. Markley, J. L., *Biological Applications of Magnetic Resonance*, Schulman R. G., Ed., Academic Press, London, 1979, chap. 9.
37. Kossiapov, A. A. and Spencer, S. A., Direct determination of the protonation states of aspartic acid-102 and histidine-57 in the tetrahedral intermediate of the serine proteases: neutron structure of trypsin, *Biochemistry*, 20, 6462, 1981.
38. Jencks, W. P., Binding energy, specificity and catalysis — the Circe effect, *Adv. Enzymol.*, 43, 219, 1975.
39. Schowen, R. L., *Transition States of Biochemical Processes*, Gandour, R. D. and Schowen, R. L., Eds., Plenum Press, New York, 1978, chap. 2.
40. Stein, R. L., Elrod, J. P., and Schowen, R. L., Correlative variations in enzyme-derived and substrate-derived structures of catalytic transition states. Implications for the catalytic strategy of acyl-transfer enzymes, *J. Am. Chem. Soc.*, 105, 2446, 1983.
41. Patterson, J. F., Huskey, W. P., Venkatasubban, K. S., and Hogg, J. L., One-proton catalysis in the intermolecular imidazole-catalyzed hydrolysis of esters and amides, *J. Org. Chem.*, 43, 4935, 1978.
42. Hubbard, C. and Kirsch, J. F., Acylation of chymotrypsin by active esters of nonspecific substrates. Evidence for a transient acylimidazole intermediate, *Biochemistry*, 11, 2483, 1972.
43. Hunkapiller, M. W., Forgacs, M. D., and Richards, J. H., Mechanism of action of serine proteases. Tetrahedral intermediates and concerted proton transfer, *Biochemistry*, 15, 5581, 1976.
44. Stein, R. L., Catalysis by human leukocyte elastase: substrate structural dependence of rate-limiting protolytic catalysis and operation of the charge-relay system, *J. Am. Chem. Soc.*, 105, 5111, 1983.
45. Quinn, D. M., Elrod, J. P., Ardis, R., Friesen, P., and Schowen, R. L., Protonic reorganization in catalysis by serine proteases: acylation by small substrates, *J. Am. Chem. Soc.*, 102, 5358, 1980.
46. Hunkapiller, M. W., Smallcombe, S. H., Whitaker, D. R., and Richards, J. H., Carbon nuclear magnetic resonance studies of the histidine residue in α -lytic protease. Implications for the catalytic mechanism of serine proteases, *Biochemistry*, 12, 4732, 1973.
47. Bachovchin, W. W. and Roberts, J. D., Nitrogen-15 nuclear magnetic resonance spectroscopy. The state of histidine in the catalytic triad of α -lytic protease. Implications for the charge-relay mechanism of peptide-bond cleavage by serine proteases, *J. Am. Chem. Soc.*, 100, 8041, 1978.
48. Westler, W. M., Markley, J. L., and Bachovchin, W. W., Proton NMR spectroscopy of the active site histidine of α -lytic protease. Effects of adjacent carbon-13 and nitrogen-15 labels, *FEBS Lett.*, 138, 233, 1982.
49. Gandour, R. D., Maggiora, G. M., and Schowen, R. L., Coupling of proton motions in catalytic activated complexes. Model potential-energy surfaces for hydrogen-bond chains, *J. Am. Chem. Soc.*, 96, 6967, 1974.
50. Eliason, R. and Kreevoy, M. M., Kinetic hydrogen isotope effect in the concerted mechanism for the hydrolysis of acetals, ketals and ortho esters, *J. Am. Chem. Soc.*, 100, 7037, 1978.
51. Küllertz, G., Oehme, P., and Barth, A., *Dipeptidylpeptidase-IV — Chemie, Biochemie und Physiologische Aspekte* (Heft II, Beiträge zur Wirkstoffforschung), Akademie-Industrie-Komplex Arzneimittelforschung, Berlin (GDR), 1981; Barth, A., Mager, H., Fischer, G., Neubert, K., and Schwarz, G., Struktur-Aktivitäts-Beziehungen bei der enzymatischen Hydrolyse von Dipeptid-Arylamiden durch Dipeptidyl-Peptidase IV, *Acta Biol. Med. Ger.*, 39, 1129, 1980.
52. Fischer, G., Heins, J., and Barth, A., The conformation around the peptide bond between the P₁ and P₂-positions is important for catalytic activity of some proline-specific proteases, *Biochim. Biophys. Acta*, 742, 452, 1983.
53. Stein, R. L., Paborji, M., and Schowen, R. L., unpublished results.
54. Hogg, J. L., Elrod, J. P., and Schowen, R. L., Transition-state properties and rate-limiting processes in the acetylation of acetylcholinesterase by natural and unnatural substrates, *J. Am. Chem. Soc.*, 102, 2082, 1980.
55. Rosenberry, T. L., Catalysis by acetylcholinesterase: evidence that the rate-limiting step with certain substrates precedes general acid-base catalysis, *Proc. Natl. Acad. Sci. U.S.A.*, 72, 3834, 1975.
56. Szawelski, R. J. and Wharton, C. W., Kinetic solvent isotope effects on the deacylation of specific acyl-papains. Proton inventory studies on the papain-catalyzed hydrolyses of specific ester substrates: analysis of possible transition-state structures, *Biochem. J.*, 199, 681, 1981.
57. Tu, C. K. and Silverman, D. N., Solvent deuterium isotope effects in the catalysis of oxygen-18 exchange by human carbonic anhydrase II, *Biochemistry*, 21, 6353, 1982.
58. Konsowitz, L. M. and Cooperman, B. S., Solvent isotope effect in inorganic pyrophosphatase-catalyzed hydrolysis of inorganic pyrophosphate, *J. Am. Chem. Soc.*, 98, 1993, 1976.
59. Welsh, K. M., Jacobyansky, A., Springs, B., and Cooperman, B. S., Catalytic specificity of yeast inorganic pyrophosphatase for magnesium ion as cofactor. An analysis of divalent metal ion and solvent isotope effects on enzyme function, *Biochemistry*, 22, 2243, 1983.
60. Wang, M.-S., Gandour, R. D., Rodgers, J., Haslam, J. L., and Schowen, R. L., Transition-state structure for a conformation change of ribonuclease, *Bioorg. Chem.*, 4, 392, 1975.

61. **Harmony, J. A. K., Himes, R. H., and Schowen, R. L.**, The monovalent cation-induced association of formyltetrahydrofolate synthetase subunits: a solvent isotope effect, *Biochemistry*, 19, 5379, 1975.
62. **Kern, D., Zaccai, G., and Giegé, R.**, Effect of heavy water substitution for water on the tRNA^{Val}-Valyl-tRNA synthetase system of yeast, *Biochemistry*, 19, 3158, 1980.
63. **Ofengand, J.**, tRNA and aminoacyl-tRNA synthetases, in *Molecular Mechanisms of Protein Biosynthesis*, Weissbach, H. and Pestka, S., Eds., Academic Press, New York, 1977, chap. 1.
64. **Khoshtariya, P. E.**, Investigation of the proton transfer in enzymatic hydrolysis by the method of temperature dependence of kinetic isotope effect. II. β -Trypsin catalyzed hydrolysis of Bz-Arg-OEt, *Bioorg. Khim.*, 4, 1673, 1978.
65. **Fujihara, H.**, unpublished data.
66. **Elrod, J. P.**, unpublished data.